Department of Materials Science and Engineering

Phase Equilibria and Thermodynamics of the System Zn-As-Cu-Pb-S at Temperatures Below 1173 K

Fiseha Tesfaye, Pekka Taskinen

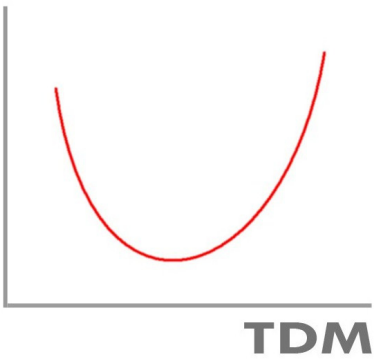

Aalto University
SCIENCE + TECHNOLOGY
RESEARCH REPORT

Fiseha Tesfaye et al. Phase Equilibria and Thermodynamics of the System Zn-As-Cu-Pb-S at Temperatures Below 1173 K Aalto University

Aalto University publication series
SCIENCE + **TECHNOLOGY** 7/2011

Phase Equilibria and Thermodynamics of the System Zn-As-Cu-Pb-S at Temperatures Below 1173 K

Fiseha Tesfaye, Pekka Taskinen

Aalto University
School of Chemical Technology
Department of Materials Science and Engineering
Thermodynamics and Modelling of Metallurgical Processes

Aalto University publication series
SCIENCE + **TECHNOLOGY** 7/2011

03.05.2011

ISBN 978-952-60-4126-1 (pdf)
ISBN 978-952-60-4125-4 (printed)
ISSN-L 1799-4896
ISSN 1799-490X (pdf)
ISSN 1799-4896 (printed)

Aalto Print
Helsinki 2011

Finland

Publication orders (printed book):
pekka.taskinen@aalto.fi, http://materials.tkk.fi/fi/tutkimusryhmat/metallurgiset_prosessit/

Boliden Harjavalta Oy, Boliden Kokkola Oy, Norilsk Nickel Finland Oy , Outotec (Finland) Oy and Tekes (the Finnish Funding Agency for Technology and Innovation)

Author
Fiseha Tesfaye, Pekka Taskinen

Name of the publication
Phase Equilibria and Thermodynamics of the System Zn-As-Cu-Pb-S at Temperatures Below 1173 K

Publisher School of Chemical Technology

Unit Department of Materials Science and Engineering

Series Aalto University publication series SCIENCE + TECHNOLOGY 7/2011

Field of research Metallurgy

Abstract

Phase relations and thermodynamics of some equilibrium phases in the systems Zn-Cu-As-S, Zn-Pb-As-S and Zn-Cu-As-Pb-S were compiled and reviewed, based on available literature. Phase relations and stabilities of some binary and ternary phases in the multi-component systems are relatively well-established. Stabilities, phase relations and solubility limits of the identified equilibrium phases were discussed. Finally, the Gibbs energies of formation of some stable phases in the system Zn-Cu-As-Pb-S and the effect of small amounts of impurities on the melting temperatures of the pure sulfides/sulfosalts and their assemblages were compiled and reviewed.

Keywords Sulfides, impurities, phase equilibria, thermodynamics

ISBN (printed) 978-952-60-4125-4 **ISBN (pdf)** 978-952-60-4126-1

ISSN-L 1799-4896 **ISSN (printed)** 1799-4896 **ISSN (pdf)** 1799-490X

Location of publisher Espoo **Location of printing** Helsinki **Year** 2011

Pages 51

Table of Contents

Symbols, Abbreviations, Units

G, (g), V	gas phase, vapor
L, (l)	liquid
P	pressure [atm]
T	temperature [^{o}C]
T_m	melting temperature [^{o}C]
T_{max}	maximum temperature of stability [^{o}C]
T_{liq}	liquidus temperature [^{o}C]
T_{sol}	solidus temperature [^{o}C]
X_i	composition of component i
ΔG^o	standard Gibbs energy [kJ/mole of a sulfosalt or sulfide]
ΔG_f	standard Gibbs energy of formation [kJ/mol of a sulfide]
ΔG_r	standard Gibbs energy of reaction [kJ/mol of a sulfide]

1 Introduction

Increasing association of impurities such as arsenic in sulfide ores has been generating flurry of both experimental studies and compilation of thermodynamic data of sulfide systems that contain both impure elements and their compounds. For instance, Zn- and Cu-sulfides are relatively common ore minerals in most hydrothermal vein and replacement deposits. Although these sulfides may occur alone or together in the absence of other sulfides, they are most commonly encountered in complex ore assemblages in which the mineralogy is significantly altered by elements such as As, Pb, or Fe [1]. Figure 1 shows a combined compositions of mainly Cu-Zn-, Zn-Pb- and Zn-Cu-sulfide ore deposits that were mined in 1970s, in southwest of Finland.

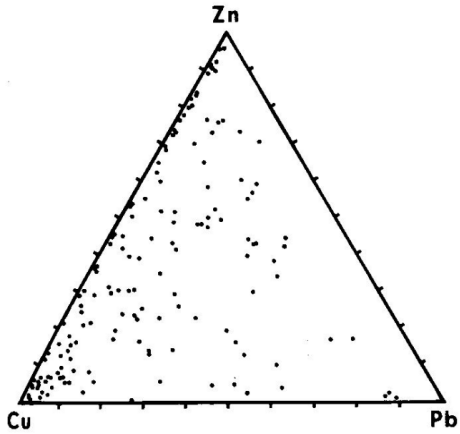

Figure 1. Metallic composition of the Aijala (Cu-Zn), Metsämonttu (Zn-Pb) and Orijärvi (Zn-Cu) sulfide ores in Zn-Cu-Pb triangular diagram [2].

Owing to the complexity of minerals in nature, a thorough evaluation of the thermochemistry of these complex ore minerals is essential for developing full understanding of the behavior of the impurities in existing and new sulfide ore minerals processing operations.

In the previous reports [3, 4, 5], the pure binary sulfides in the (Fe, Ni, Cu, Zn)-S systems and their ternaries as well as the phase equililibria and thermodynamic properties of the (Ni, Cu)-(As, Sb)-S, Cu-Bi-S and Zn-As-S systems were discussed. The main purpose of this study was to review the stable phase relations and thermodynamics of the Zn-As-(Cu, Pb)-S systems. The intention was to contribute to the evaluation of the behavior of impurities in zinc minerals processing operations, at 'pre-roasting conditions'.

2 Phase Equilibria and Thermodynamics

In this chapter, the phase equilibria and thermodynamics of the systems Zn-Cu-As-S, Zn-Pb-As-S and Zn-Cu-As-Pb-S are reviewed, based on the available literature. Thermodynamic data for the available reactions of formation are summarized in chapter 3. Some of the sulfide systems reviewed in the previous reports [3, 4, 5] are included either to emphasis important features or supplement the reports.

2.1 The System Zn-*Cu-As*-S

In this section, phase equilibria and thermodynamics of the systems As-S, Zn-As, Zn-As-S, Cu-As-S, Zn-Cu, Zn-Cu-S and Zn-Cu-As-S will be discussed.

2.1.1 As-S

Phase relations in the As-S system were reviewed in the previous reports [4, 5]. In this study, only the liquid and gas phases are considered. Thermodynamic data for equilibrium phases in the system are summarized in chapter 3.

Using the $Fe_{1-x}S$ as an indicator for the chemical potential of sulfur, Barton [6] evaluated the thermochemistry of the As-S liquids at temperatures between 266.85 - 816.85 ^{o}C. Results of his evaluation are shown in Figure 2. This information coupled with the Gibbs-Duhem equation could be used to predict activities of As in the As-S melts.

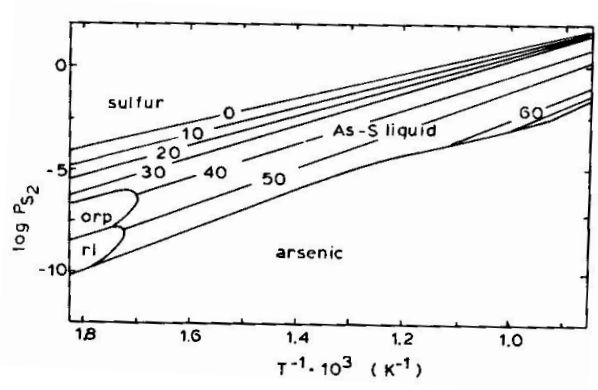

Figure 2. Experimental data showing the partial pressure of S_2 (g) in equilibrium with the As-S melts as a function of inverse temperature. Isopleths represent at. % As in the melts. The symbols orp and rl refer to minerals orpiment and realgar, respectively [6].

2.1.2 Zn-As

Among the base metals, Zn melts and boils at relatively lower temperatures of 419.58 °C and 927 °C, respectively [7]. Arsenic melts at 814, at 36 atm., and sublimes at 615 °C at 1 atm. [8]. Equilibrium phases in this system are liquid, L, rhombohedral terminal solid solution (As), monoclinic As_2Zn, β-, α'-, and α-As_2Zn_3 and the hexagonal terminal solid solutions, (Zn). The boundaries on the As-rich side, shown in Figure 3, were measured under unspecified pressures higher than 1 atm. As_2Zn dissociates incongruently into As_2Zn_3 and As_4(g). According to Heike [9], the dissociation pressure can be expressed by equation (1).

$$\log(P(atm)) = 16.1841678/T + 0.01973679 \quad (1)$$

The homogeneity range of As_2Zn_3 is narrow [9]. More precisely, the solubility of As in β-As_2Zn_3 is at least 0.002 at. % at 672 °C and it does not exceed 0.0005 at. % in α-As_2Zn_3 [10]. The L ⇌ As_2Zn_3 + (Zn) eutectic temperature and the melting point of Zn are essentially the same [9, 11].

Pietraszko and Łukaszewicz [12], and Clark and Range [13] determined the pressure-temperature diagram of As_2Zn up to 42 Kbar. The melting point of As_2Zn decreased from 723 °C at ambient pressure to 679 °C at 19.0 Kbar. Clark and Range [13] found that AsZn forms as a decomposition product of As_2Zn at high pressures and temperatures and also by a reaction As_2Zn_3 + As ⇌ 3AsZn at 40 Kbar and 800 to 1200 °C.

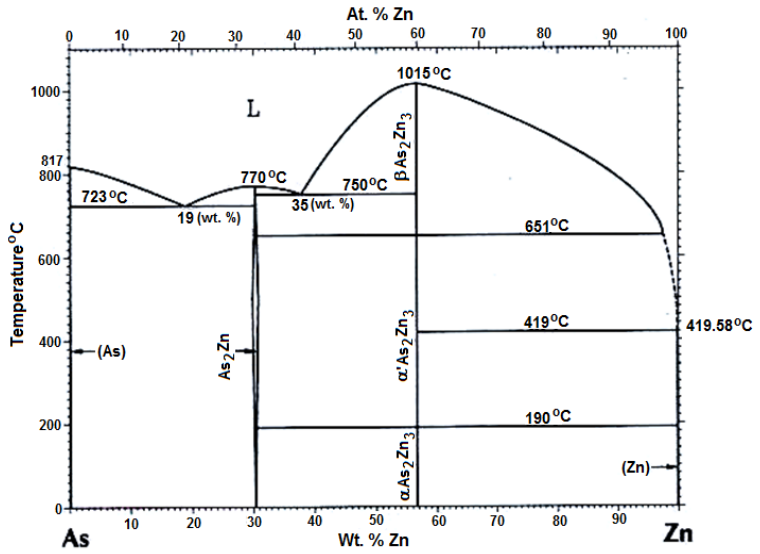

Figure 3. The Zn-As phase diagram (Okamoto, 1992) [15].

Schoonmaker and Lemmerman [14] used a torsion effusion method over a temperature range of 335.85 to 579.85 °C to evaluate the reaction:

$$Zn_3As_2(s) = 3Zn(g) + ½As_4(g) \quad (2)$$

In their analysis, they accounted for the dissociation of tetrametric arsenic vapor to the dimer:

$$As_4(g) = 2As_2(g) \quad (3)$$

Based on their experimental data, the Gibbs energy for the formation of Zn_3As_2 is calculated as shown in Figure 4.

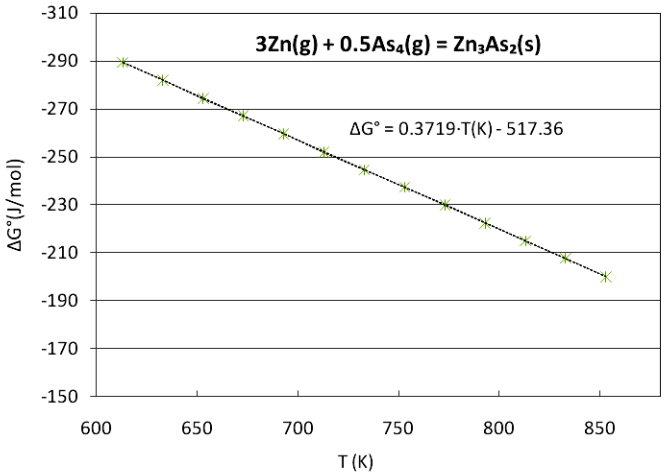

Figure 4. The Gibbs energy vs. T for the formation reaction of the Zn_3As_2, data from Schoonmaker and Lemmerman [14].

2.1.3 Zn-As-S

The controversial dissolution of As in ZnS has been under a debate in the 1950s and 60s. While studying the mineralogical complex in the Pampa Larga mining district of northern Chile, Alan (1970) [16] described the occurrence of arsenic bearing sphalerite. The possibility that the arsenic might be present as discrete inclusions of realgar or orpiment (As_2S_3) was investigated by electron-probe microanalysis of several intergrown crystals. Arsenic was confirmed as a constituent of the sphalerite, and no inclusions of arsenic sulfides were detected. Wavelength scanning across each of the crystals showed that the arsenic is homogeneously distributed. An arsenic content of 1.7 ± 0.3 wt. % was determined using the associated realgar (assumed to be stoichiometric AsS) as a standard. In *in vacuo* heating experiments, the arsenian sphalertite decomposed to a honey like-yellow sphalerite and probable realgar after four hours of heating at 200 °C, but

persisted without a change in color or in cell edge at 150 °C for 32 hours. Annealing in the presence of magnesium metal for 42 hours at 150 °C resulted in no increase in cell edge (Skinner and Barton, 1960 [17]), so the arsenian sphalerite is apparently free of oxygen. Furthermore, Frondel (1967) [18] claimed that the response of this phase to heating suggests the presence of no organic compounds. Sphalerites in equilibrium with FeAsS, pyrite (FeS_2) and native As do not contain As (i.e. < 0.001 wt. % As), which may suggest that the dissolution of As in sphalerite is prevented by even a minor amount of Fe.

Based on his investigation, Alan [16] concluded that for T < 200 °C, Zn (As, S) is probably a stable phase in the Zn-As-S system. Above 200 °C it decomposes as follows;

$$Zn\ (As, S) \xrightarrow{T > 200^{\circ}C} ZnS + AsS \qquad (4)$$

After annealing at 350 °C for 192 hours, Shie et al. [20] examined an interface between thin layers of compositions $As_{50}S_{50}$ and Zn. They used EPMA (electron probe microanalysis) line scan to determine the composition of reaction products through the interface and reported existence of a homogenous phase $As_{21}S_{23}Zn_{56}$. However, they didn't make any sub-micron level examinations by using TEM/SEM or XDR for possible appearance of a homogenous two-phase sub-micron mixtures as a single phase; thus, they suggested further studies to confirm the existence of the equilibrium ternary phase, $As_{21}S_{23}Zn_{56}$.

Experimental phase equilibrium studies on the broader Zn-As-S system are very limited. The only laboratory study, by Olekseyuk and Tovtin [19], using synthetic phases showed that synthesis of alloys along the ZnS-As_2S_5 join to not result in formation of any ternary phase.

The Zn_3As_2-ZnS phase diagram, shown in Figure 5, is peritectic at 10.5 mol. % ZnS. The solubility of ZnS in β-Zn_3As_2 at the peritectic temperature is ~16 mol. % ZnS and falling to 7 mol. % ZnS at 610 °C and to 1 mol. % ZnS at 240 °C. The equilibrium diagrams of the $ZnAs_2$-ZnS, As-ZnS, As_2S_2-ZnS and As_2S_3-ZnS sections are eutectic at 0.5, 0.7, 0.9 and 3 mol. % ZnS and at 761.85, 785.85, 301.85 and 299.85 °C, respectively.

Generally, there are nine phase crystallization fields in the Zn-As-S system: ZnS, β-solid solutions based on Zn_3As_2, α-solid solutions based on Zn_3As_2, $ZnAs_2$, As, As_2S_2, As_2S_3, S and Zn. Seven invariant equilibria points observed by Olekseyuk and Tovtin [19] are listed in Table 1. At 226.85 °C, a homogeneous single phase region exists only around the Zn_3As_2 corner.

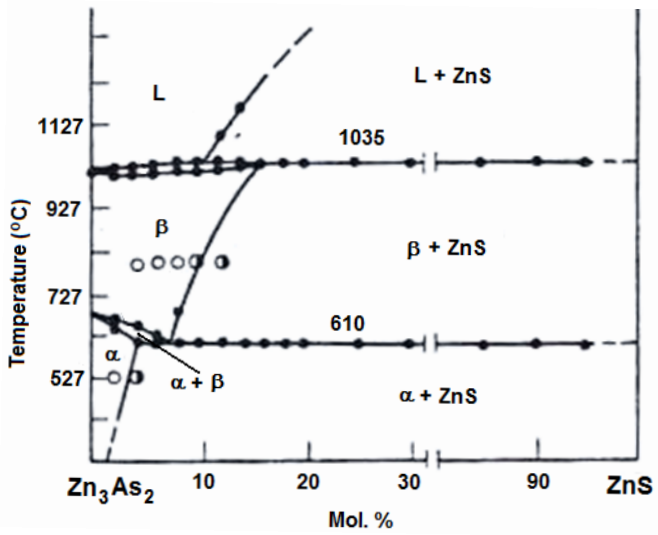

Figure 5. Phase diagram of the pseudo-binary Zn_3As_2-ZnS system [19].

Table 1. Invariant processes which take place in the Zn-As-S system [19].

Reaction	Temperature(°C)
L ⇌ZnS+ β-Zn_3As_2 + Zn	416.85
L ⇌ ZnS + $ZnAs_2$ + As	664.85
L ⇌ ZnS + As_2S_2 + As	289.85
L ⇌ ZnS + As_2S_2 + As_2S_3	274.85
L ⇌ ZnS + As_2S_3 + S	~99.85
L + β-Zn_3As_2⇌ α-Zn_3As_2 + Zn	417.85
L + ZnS ⇌ β-Zn_3As_2+ $ZnAs_2$	759.85

2.1.4 Cu-As-S

The first melt in the system Cu–As–S appears on the assemblage β-S_8-As_2S_3-CuS at about 114 °C [21]. This melt remains Cu-poor until around 500°C; above this temperature, increase in temperature causes the field of liquid to expand to more Cu-rich compositions (Figure 6). Tennantite ($Cu_{12.31}As_4S_{13}$) and enargite (Cu_3AsS_4), the major ternary minerals in this system, melt at about 665 and 671°C (Maske & Skinner [22]), respectively. Thermodynamic data for some of the ternary compounds are given in chapter 3 and a summary of the ternary phases that are reported by different investigators and peritectic and melting reactions are given in appendix and Table 2, respectively.

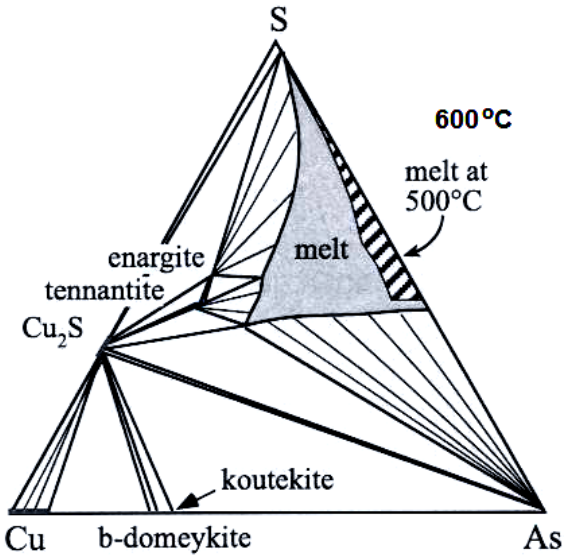

Figure 6. A one bar phase relations in the Cu–As–S system at 600°C [23]. Ruled fields show the size of the melt fields in this system at 500°C and one bar; the data were taken from Skinner et al. (1972) [24] and Maske & Skinner (1971) [22].

Table 2. Non-variant reactions in the system Cu-As-S [21].

Reaction	T (°C)	Reaction type
$L \rightleftarrows (Cu_{3-x}As(HT)) + (Cu_{2-x}S)$	800	eutectic
$L \rightleftarrows (Cu_{2-x}S) + (As)$	714	eutectic
$L + (Cu_{3-x}As(HT)) \rightleftarrows (Cu_{5-\delta}As_2(HT)) + (Cu_{2-x}S)$	708 ?	half eutectic
$L_1' \rightleftarrows L_1'' + (As) + (Cu_{2-x}S)$	700 ?	ternary monotectic
$L \rightleftarrows (Cu_{3-x}As(HT)) + (Cu) + (Cu_{2-x}S)$	680 ?	ternary eutectic
$L \rightleftarrows Cu_3AsS_4$	672	congruent
$L \rightleftarrows Cu_{12+x}As_{4+y}S_{13}$	656	congruent
$L \rightleftarrows Cu_3AsS_4 + (Cu_{2-x}S)$	655 ?	eutectic
$L \rightleftarrows Cu_3AsS_4 + Cu_{12+x}As_{4+y}S_{13}$	655 ?	eutectic
$L \rightleftarrows (Cu_{2-x}S) + Cu_{12+x}As_{4+y}S_{13}$	650	eutectic
$L \rightleftarrows Cu_{12+x}As_{4+y}S_{13} + (Cu_{2-x}S) + Cu_3AsS_4$	645 ?	ternary eutectic
$L \rightleftarrows (Cu_{5-\delta}As_2(HT)) + (As) + (Cu_{2-x}S)$	599 ?	ternary eutectic
$L + (Cu_{2-x}S) \rightleftarrows Cu_{12+x}As_{4+y}S_{13} + (As)$	598	half eutectic
$L + Cu_{12+x}As_{4+y}S_{13} \rightleftarrows Cu_4As_2S_5$	597	peritectic
$L + Cu_{12+x}As_{4+y}S_{13} + (As) \rightleftarrows CuAsS$	574	ternary peritectic
$L + Cu_{12+x}As_{4+y}S_{13} \rightleftarrows Cu_3AsS_4 + Cu_4As_2S_5$	573	half eutectic
$(As) + Cu_{12+x}As_{4+y}S_{13} \rightleftarrows (Cu_{2-x}S) + CuAsS$	571	half eutectoid
$L_5' \rightleftarrows L_5'' + Cu_3AsS_4 + (Cu_{2-x}S)$	550 ?	ternary monotectic
$L + Cu_4As_2S_5 \rightleftarrows Cu_6As_4S_9$	530	peritectic
$L + (Cu_{2-x}S) \rightleftarrows (CuS) + Cu_3AsS_4$	507 ?	half eutectic
$(Cu_{2-x}S) + (Cu_{3-x}As(HT)) \rightleftarrows (\beta\text{-}Cu_2S)$	498	peritectoid
$L + Cu_{12+x}As_{4+y}S_{13} \rightleftarrows Cu_4As_2S_5 + CuAsS$	474	half eutectic
$L + Cu_4As_2S_5 \rightleftarrows Cu_6As_4S_9 + CuAsS$	470 ?	half eutectic
$L + Cu_4As_2S_5 \rightleftarrows Cu_3AsS_4 + Cu_6As_4S_9$	456	half eutectic
$L \rightleftarrows CuAsS + (\beta\text{-}As_4S_4)$	316 ?	eutectic
$L \rightleftarrows (As_2S_3) + Cu_6As_4S_9$	309	eutectic
$L + Cu_6As_4S_9 \rightleftarrows Cu_3AsS_4 + (As_2S_3)$	306 ?	half eutectic
$L + CuAsS \rightleftarrows Cu_6As_4S_9 + (\beta\text{-}As_4S_4)$	280 ?	half eutectic
$L \rightleftarrows Cu_6As_4S_9 + (\beta\text{-}As_4S_4) + (As_2S_3)$	270 ?	ternary eutectic
$L \rightleftarrows (As) + (\alpha\text{-}As_4S_4) + CuAsS$	195 ?	ternary eutectic
$L + Cu_3AsS_4 \rightleftarrows (As_2S_3) + (CuS)$	180 ?	half eutectic
$L \rightleftarrows (\beta\text{-}S_8) + (CuS) + (As_2S_3)$	114 ?	ternary eutectic

2.1.5 Zn-Cu

Assessed phase diagrams of the Cu-Zn system are shown in Figure 7 and Figure 8, and reactions at the special points are given in Table 3.

Thermodynamic functions of solid alloys as summarized by Hultgren and Desai [25], based on EMF measurements, are shown in Table 4.

Maximum solid solution of Zn in Cu (α -phase) is 38.3 at. % (39.0 wt. %) and occurs at 454 °C. Maximum solid solution of Cu in Zn (η-phase) is 2.77 at. % (2.7 wt. %) and occurs at 424 °C. Additional Cu-Zn phases are the β-phase (stable below 902 °C and containing a maximum of about 57 wt. % Zn at 834°C and a minimum of about 38 wt. % Zn at 902 °C); the γ-phase (stable below 834 °C and with maximum extent of solid solution at 558 °C where it spans the region from 57 to 70 wt. % Zn); the δ-phase (stable between 558 ° and 700 °C, with maximum solid solution from about 74 to 77 wt % Zn at 598 °C); and the ε-phase (stable below 598 °C, with maximum solid solution from about 79 to 87 wt % Zn at 424 °C). The β-, γ-, δ- and ε-phases all melt incongruently as follows:

β-, γ-, δ- and ε-phase → $Cu\text{-}Zn_{(s)}$(Cu-rich) + $Zn\text{-}Cu_{(l)}$(Zn-rich) (5)

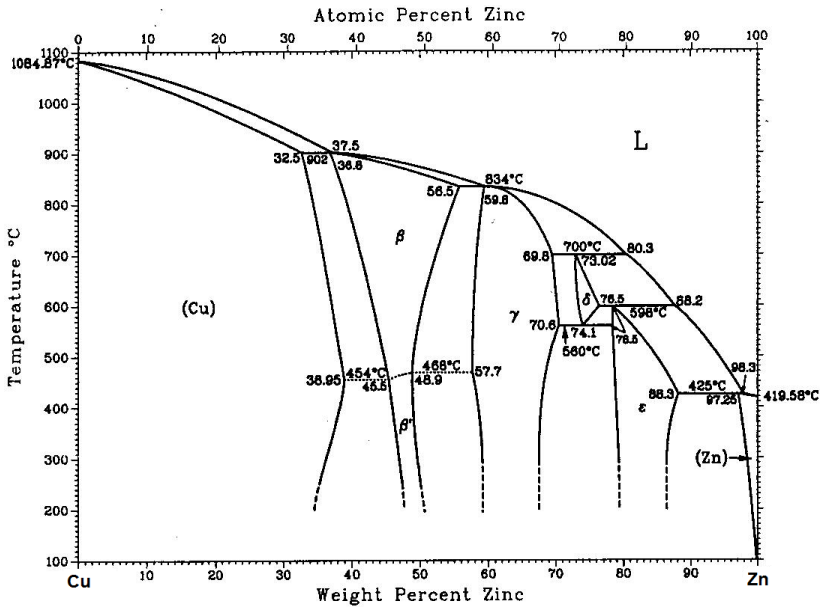

Figure 7. The Cu-Zn system. α: 0 - 38.3 at.% Zn, β: 36.1 - 59.1 at.% Zn, β': 44.7 - 48.2 at.% Zn, γ: 57 - 70.0 at.% Zn, δ: 72.5 - 76.0 at.% Zn, ε: 78.0 - 88.0 at. % Zn, η: 97.2 - 100 at.% Zn [26].

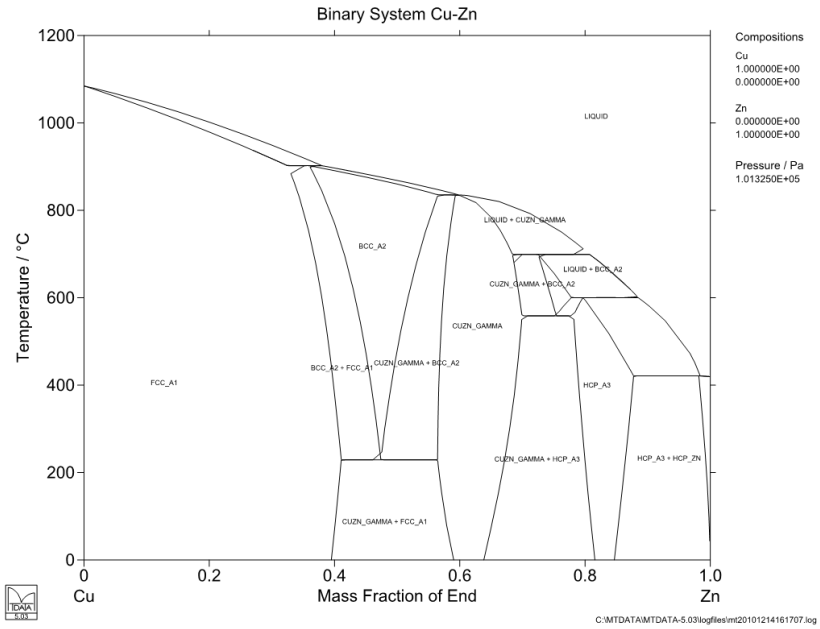

Figure 8. Phase diagram of the system Cu-Zn. Calculated by MTDATA software (Davies et al. 2002) version 5.03 [27] using MTOX database (Gisby et al. 2007) version 6 [28].

Table 3. Peritectic and eutectoid reactions in the Cu-Zn system [29].

Reaction	Composition (at. % Zn)	T (°C)	Reaction type
$\alpha + L \leftrightarrow \beta$	36.1 – 36.8	902	peritectic
$\beta + L \leftrightarrow \gamma$	59.1	834	peritectic
$\gamma + L \leftrightarrow \delta$	72.45 – 79.8	700	peritectic
$\delta + L \leftrightarrow \varepsilon$	78.0 – 87.9	598	peritectic
$\varepsilon + L \leftrightarrow \eta$	97.17 – 98.25	425	peritectic
$\delta \leftrightarrow \gamma + \varepsilon$	70.0 – 78.0	560	eutectoid

Table 4. Integral quantities for solid alloys at 326.5 °C ($Cu_{0.525}Zn_{0.475}$(s)) and 500 °C ($Cu_{1-x}Zn_x$(s)) [25].

(1-x)Cu(s) + xZn(s) = $Cu_{1-x}Zn_x$(s)					500 °C	
X_{Zn}	Phases & crystal structures	ΔG (cal/ g-atom)	ΔH(cal/ g- atom)	ΔS(cal/ g-atom·K)	ΔG^{xs}(cal/ g- atom)	ΔS^{xs}(cal/ g-atom·K)
0.1	(Cu)(fcc)	- 1111	- 627	0. 626	- 612	- 0.020
0.2		-1896	- 1309	0.759	- 1127	- 0.235
0.3		- 2419	- 1754	0.861	- 1481	- 0.353
0.381		-2677 (± 300)	-1969 (± 150)	0.916 (± 0.4)	- 1657 (± 150)	-0.404 (± 0.4)
0.44	β (bcc(A2))	- 2815	- 2112	0.909	- 1761	- 0.454
0.45		- 2837	- 2141	0.900	- 1780	- 0.467
0.47		- 2873	- 2199	0.872	- 1811	- 0.502
0.488		- 2896 (±200)	-2251 (±300)	0.834 (± 0.5)	- 1832 (± 200)	-0.542 (± 0.5)
0.582	γ(bcc($D8_2$))	- 2995	- 2625	0.479	- 1951	- 0.872
0.6		- 3026	- 2726	0.388	- 1992	- 0.949
0.65		- 2917	-2718	0.257	- 1922	- 1.030
0.672		- 2805	- 2588	0.281	- 1832	- 0.978
0.761	ϵ (hcp(A3))	- 2267	- 2050	0.281	- 1422	- 0.813
0.80		- 2007	-1836	0.221	- 1238	- 0.773
0.82		- 1854	- 1700	0.199	- 1130	- 0.738
0.847		- 1627	- 1484	0.185	- 969	- 0.666
0.525Cu(s) + 0.475Zn(s)= $Cu_{0.525}Zn_{0.475}$(s)					326.5 °C	
0.475	β'(bcc(B2))	-2755 (± 200)	-2657 (± 300)	0.164 (± 0.6)	-	-

2.1.6 Zn-Cu-S

The only compound that exists in the Zn-S binary system is ZnS. It exhibits both polymorphism and polytypism at ambient pressure. Sphalerite, wurtzite and the wurtzite polytypes all have structures based on the closest packing of their constituent atoms. The Zn and S atoms form interleaved stacking sequences of closest-packed layers, and Zn is in four-fold tetrahedral coordination with sulfur. Pure sphalerite structure ZnS sublimes at 1185 °C and melts congruently at 1830 °C and 3.7 atm [30].

At ambient pressure, the transformation temperature for the polymorphs lies between 1013 to about 1130 °C, based on whether the phase is enriched with Zn or S. Furthermore, Scott et al. [31] maintained that wurtzite is sulfur-deficient relative to the sphalerite and both minerals have a combined non-stoichiometry in the order of 0.9 at. %.

Wiggins and Craig [32] suggested that most natural sphalerites, which are assumed to have equilibrated above 400 °C, coexisting with pyrite, pyrrhotite and chalcopyrite contain < 0.5 wt. % CuS. The experimental work of Craig and Kullerud [1] in evacuated silica tubes has also shown that the solid solution of Cu_2S in ZnS at 500 °C is less than 1 wt. %. Scott (1983) [33] has also claimed that the solubility of CuS in the ZnS to be < 1 at. %, at temperatures below 600 °C.

A naturally occurring ternary phase Cu_3ZnS_4 was reported by Clark and Sillitoe [34], however the work of Craig and Kullerud (1973) [1] at 1000 °C, 800 °C, 500 °C and 400 °C, didn't confirm that. Thus, the ternary phase may be stable or metastable only at temperatures below 200 °C. However, Craig and Kullerud (1973) [1] found that up to 7 wt. % Zn enters the high-temperature chalcocite-digenite solid solution. The observed solid solubility of copper in sphalerite, however, did not exceed one percent, even at 800 °C [1, 35]. The isotherms at 1000 °C, 800 °C, and 500 °C are shown in Figure 9, Figure 10 and Figure 11. In all isotherms the high stability of ZnS compared to Cu_2S were manifested.

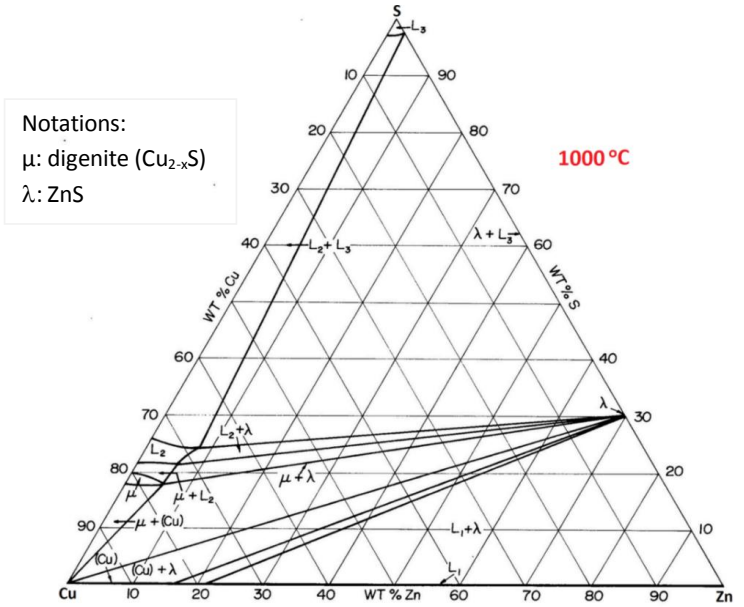

Figure 9. Phase relations in the Cu-Zn-S system at 1000 °C [37].

Moh (1960) [36], on the other hand, had previously reported the formation of small amounts of an optically distinctive phase in association with covellite, in an experimental study of the CuS - ZnS join at 400°C. By analogy with "idaite (Cu_5FeS_6)," a composition of Cu_5ZnS_6 was tentatively assigned to this product. Two other, even less well-defined, phases were also observed [34].

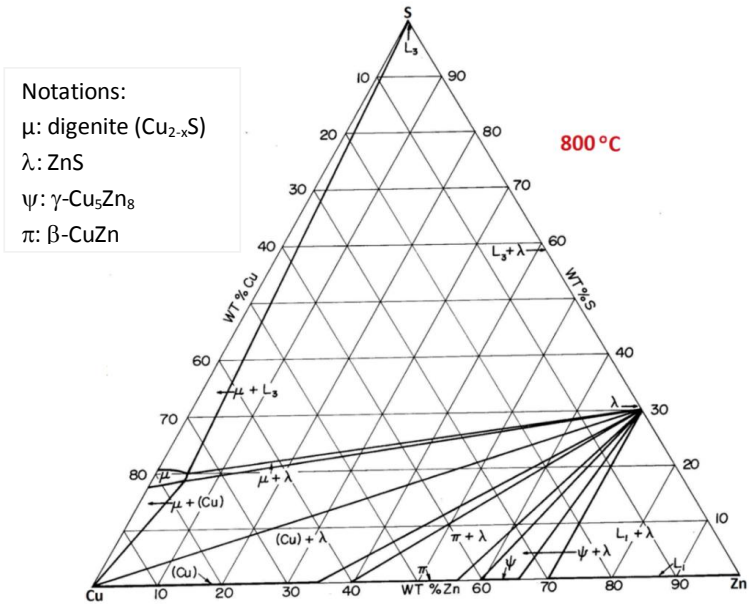

Figure 10. Phase relations in the Cu-Zn-S system at 800 °C [37].

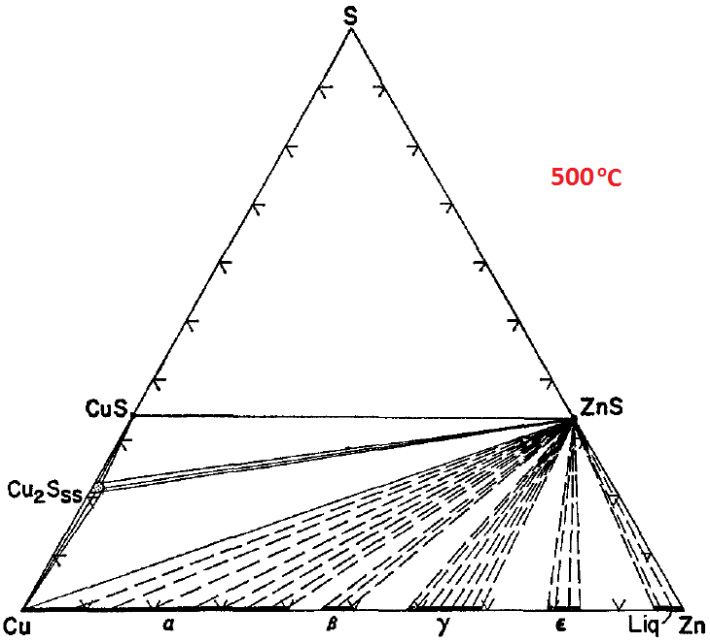

Figure 11. Phase relations in the Cu-Zn-S system at 500 °C, compositions are in wt. % [1].

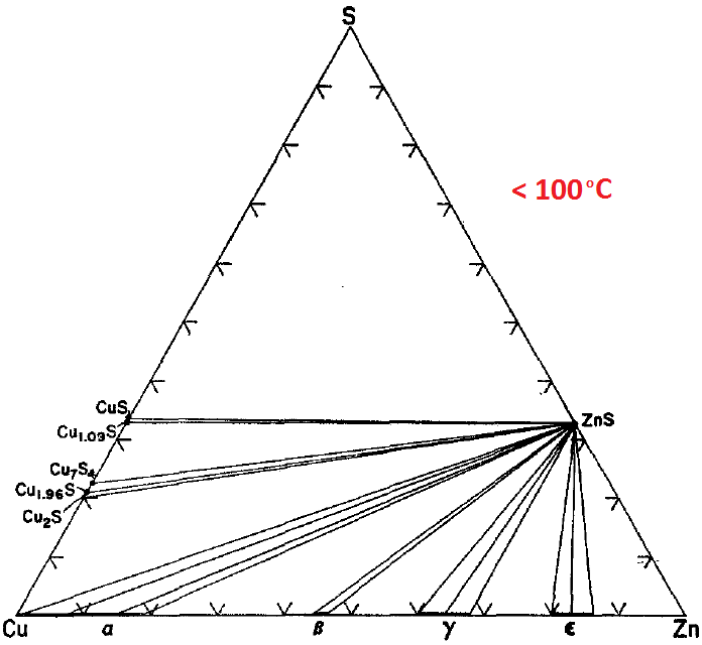

Figure 12. Stable mineral assemblages in the Cu-Zn-S system at low temperature, compositions are in wt. % [1].

2.1.7 Zn-Cu-As-S

This system comprises a four-component phase, identified as mineral nowackiite: $Cu_6Zn_3As_4S_{12}$. Craig and Barton [38] estimated its energy of formation at about the room temperature, as presented in chapter 3 (Table 11 and Table 12). This copper-zinc arsenosulfosalt has a defect zincblende-type structure, where the S atom positions on three-fold rotation axis being vacant [39]. The Cu-rich mineral described by Robert et al. [40]; Zn-tenanntite ($Cu_{10}Zn_2As_4S_{13}$), as discussed in the previous report [5], is also a quaternary phase of this system. Compilations of its formation energies are given in chapter 3 (Table 11).

2.2 The System Zn-*Pb-As*-S

In this section, phase equilibria in the systems Pb-S, Pb-As, Pb-As-S, Zn-Pb and Zn-Pb-S will be discussed. The equilibrium assemblages; native chemical elements, binary- and ternary-phases, and their solubility into one another will be discussed. At temperatures below 900 °C, there are no quaternary equilibrium phases, in the four-component system, reported to exist as a mineral or synthetic phase. Furthermore, no experimental phase equilibria studies in the broader quaternary system are available in the literature.

2.2.1 Pb-S

At a standard pressure condition, Pb melts at 327 °C [23] and S melts at 115.22 °C [41]. The system Pb-S is known to have only one compound, PbS, which is also known as a mineral galena. Galena, which is the fourth most common sulfide mineral, melts congruently at 1115 °C [42]. A silica-glass tube quenching experiments of Kullerud [42], in the presence of excess sulfur, have shown that PbS melts already at about 830 °C. Some of the results reported are shown in Table 5. A phase diagram of the system is depicted in Figure 13.

Table 5. Reactions of PbS and S at three different temperatures.

Reaction	wt. % PbS	T(°C)	Time/hours
PbS + S = PbS + S(l)	53.4	700	8
PbS + S = PbS-rich(l) + S(l)	50	830	0.5
PbS + S =L	85	850	0.5

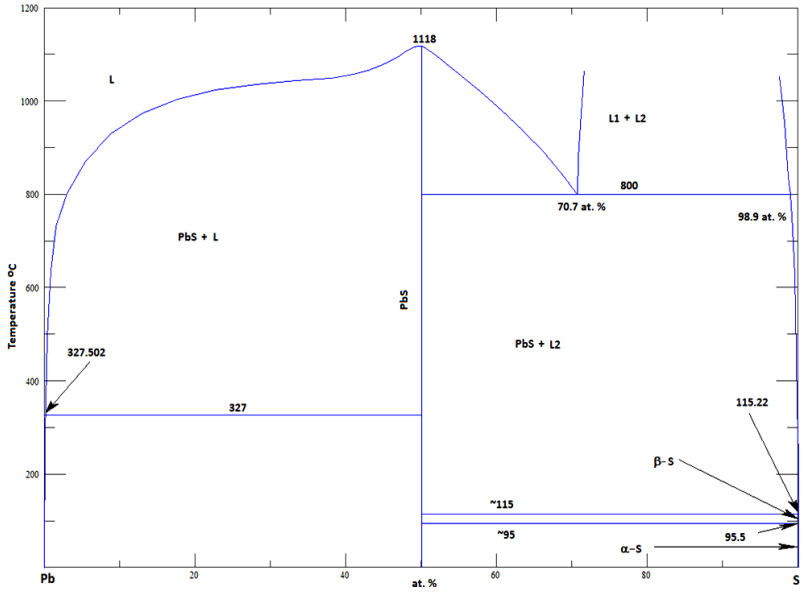

Figure 13. Phase diagram of the system Pb-S, assessed based on 43 available sources [41].

2.2.2 Pb-As

Hansen and Anderko [43] have compiled the phase diagram studies up to 1958. Critical analysis and optimization by Rannikko et al. [44] and reviews by Schlesinger and Lynch (1985) [45] and Gokcen [21] compiled the thermodynamic properties of one molten and solid As-Pb alloys.

As shown in Figure 14 and Figure 15, this system does not have any intermediate phase. The liquid phase, L, and the solid phases (αAs) and (Pb) are the equilibrium phases of this system in 1 bar. Both contain very small amounts of dissolved coexisting phases. The assessed phase diagram, shown in Figure 15, is at 1 atm up to 70 at. % As, above which pressure of gaseous As is higher. High pressures up to 36 atm are not expected to affect the liquidus [46]. The eutectic composition is nearly independent of pressure, but the eutectic temperature (291 °C) increases to 337.9 °C at 10 Kbar and 421.8 °C at 35 Kbar [46]. Solid solubilities up 100 °C are immeasurably small [47]. The solid solubility of Pb in (As) is very small [48] and is estimated to be less than 0.1 at. % Pb in the assessed diagram. Heike [48] determined the liquidus line for alloys with as high as 82.3at. % As, which is the highest As concentration in As-Pb melts studied experimentally.

The critical analysis of Rannikko et al. [44] on the thermodynamic properties of solid and liquid As-Pb alloys suggested the following eutectic points: T: 292.49 and ${}^{fcc}x_{As}$=0.00150, ${}^{e}x_{As}$=0.0664 and ${}^{rho}x_{As}$=1.0000. Their optimized As-Pb phase diagram with experimental points is shown in Figure 14.

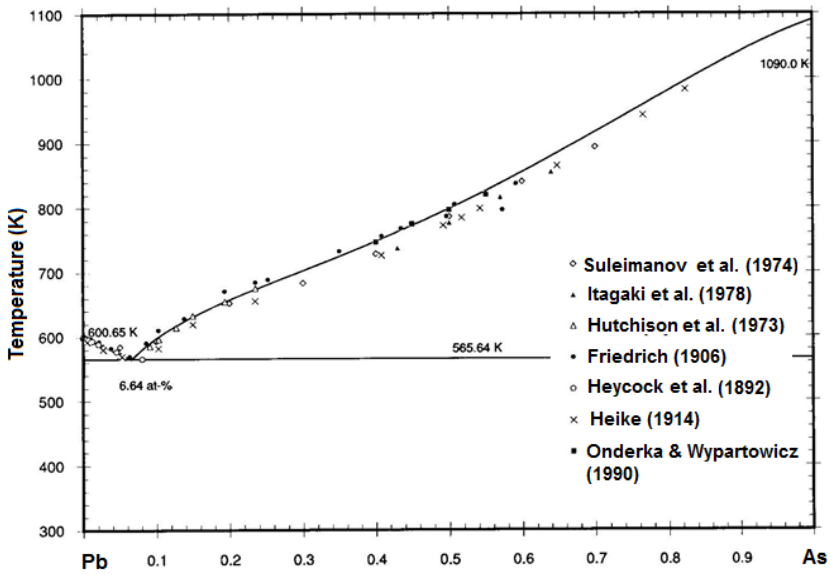

Figure 14. Optimized As-Pb phase diagram with experimental points [44].

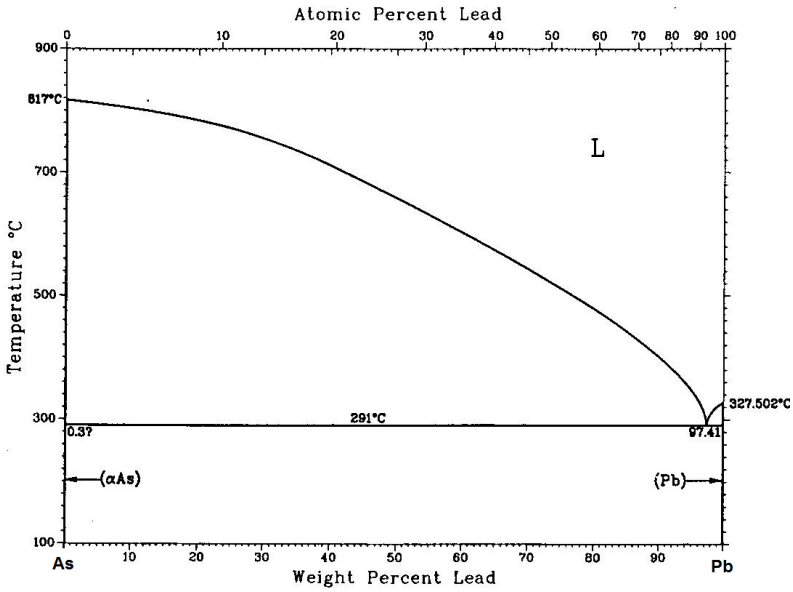

Figure 15. An assessed phase diagram of the As - Pb system [26].

Schlesinger and Lynch (1985) [45] reviewed the available literature on the thermochemistry of the molten Pb-As system. They concluded that the results obtained in two EMF studies conducted by Zaleska [49] and Suleimanov et al. [50] are the most extensive works in the area, and their data are suitable for extrapolation to conditions employed in other investigations. Consequently, they used a least squares technique to fit the data of Zaleska [49] and Suleimanov et al. [50] to the subregular equations:

$$\ln\gamma_{Pb} = X_{As}^2 / RT\cdot[2\cdot X_{Pb}\cdot A_{As\text{-}Pb} + (1 - 2\cdot X_{Pb})\cdot A_{Pb\text{-}As} + X_{Pb}\cdot(2 - 3\cdot X_{Pb})\cdot A_{As\text{-}As}]$$

and

$$\ln\gamma_{As} = X_{Pb}^2 / RT\cdot[2\cdot X_{As}\cdot A_{Pb\text{-}As} + (1 - 2\cdot X_{As})\cdot A_{As\text{-}Pb} + X_{As}\cdot(2 - 3\cdot X_{As})\cdot A_{As\text{-}As}] + C$$

where C in the last equation is an integration constant. Normally is zero when integration of the Gibbs-Duhem equation is started at $X_{As} = 1$. The normal procedure for the integration of the Gibbs-Duhem equation could not be used by Schlesinger and Lynch (1985) [45] as that would have involved integrating the Gibbs-Duhem equation, which contains the constants $A_{As\text{-}Pb}$, $A_{Pb\text{-}As}$ and $A_{As\text{-}As}$ over an extended composition range for which the constants may not apply. Values of the integration constant and the subregular solution parameters, $A_{As\text{-}Pb}$, $A_{Pb\text{-}As}$ and $A_{As\text{-}As}$, are listed in Table 6.

Table 6. Sub-regular solution parameters and integration constant for the molten Pb-As system, with respect to a liquid standard state for both As and Pb [45].

T(K)	C	A_{As-Pb}	A_{Pb-As}	A_{As-As}
Suleimanov et al. [50]				
776	- 737	1180	514	- 689
855	- 571	1136	769	- 571
913	- 310	1110	959	- 755
976	- 178	1080	1170	- 791
Zaleska [49]				
776	- 852	1030	768	135
855	- 634	558	976	454
913	- 369	216	1150	658
976	- 133	- 178	1280	979

2.2.3 Pb-As-S

By using the silica-tube quenching experiments and gold-tube pressure experiments, to study the effect of pressure on the reaction: $Pb_9As_4S_{15}$ = PbS + L, Roland [51] studied phase relations in the PbS-rich portion of the system Pb-As-S. His studies showed that Jordanite, $Pb_9As_4S_{15}$, is stable below 549 ± 3 °C, the temperature at which it melts to PbS + L + V (S-rich). In the study, confining pressures of up to 2 Kb did not measurably change the temperature of this reaction. Results of the silica-tube experiments for determining the composition of jordanite are shown in Table 8. In the presence of Sb Jordanite ($Pb_{16-x}As_{12}S_{14-x}$, where $0.8 < x < 1.4$) may convert to the isostructural geocronite ($Pb_{28-x}(As,Sb)_{12}S_{46-x}$), as a result of an extensive substitution reaction [51].

The available phase diagrams of the binary As_2S_3-PbS and ternary Pb-As-S systems are shown in Figure 16 and Figure 17, respectively. As shown in Figure 16, there are five sulpharsenides in this system. All except dufrenoysite show incongruent melting, forming the next PbS-rich phase + liquid. The heating experiment done by Roland (1968) [51] showed that gratonite is a low temperature dimorph of jordanite. The inversion temperature is below 250 °C.

Experimental works on this system, up to 1972, was critically reviewed by Chang and Bever [52]. They have shown that the composition of baumhaueterite was highly disputed, and gratonite and jordanite are

different phases with different compositions rather than polymorphs. Some minerals reported to occur naturally are listed in Table 7.

Table 7. Lead sulfosalt minerals reported to exist in nature [52, 53].

Mineral name	Composition	Ref.
Sartorite	$PbAs_2S_4$	[52, 53]
Baumhaueterite	$Pb_4As_6S_{13}$	
Rathite	$Pb_3As_4S_9$	[52]
Rathite III	$Pb_3As_5S_{10}$	[53]
Rathite Ia	$Pb_7As_9S_{20}$	
Dufrenoysite	$Pb_2As_2S_5$	[52, 53]
Jordanite	$Pb_{27}As_{14}S_{48}$	[52]
Gratonite	$Pb_9As_4S_{15}$	
Liveingite	$Pb_{18.5}As_{25}S_{56}$	[53]
	$Pb_5As_8S_{17}$	[52]

According to Pring (1990) [53] sartorite ($PbAs_2S_4$), rathite III ($Pb_3As_5S_{10}$), baumhaueterite ($Pb_4As_6S_{13}$), liveingite ($Pb_{18.5}As_{25}S_{56}$) and dufrenoysite ($Pb_2As_2S_5$) are a well-characterized minerals.

The first melt in the system Pb–As–S forms at 305°C and has only a small fraction of Pb. The melt becomes progressively richer in Pb with increasing temperature. Above 600 °C, all of the Pb–As sulfosalts are melted, and a ternary Pb–As–S melt coexists with galena.

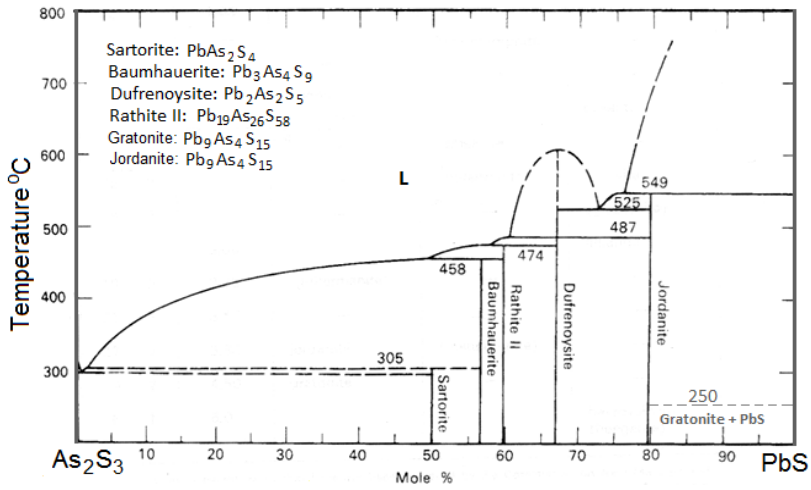

Figure 16. Phase relations in the binary As_2S_3-PbS system (modified from Kutoglu (1969) [54] with gratonite/Jordanite transformation temperature, taken from Roland (1968) [51]), compositions are rough estimates based on both compositions in the diagram and reported minerals and compounds.

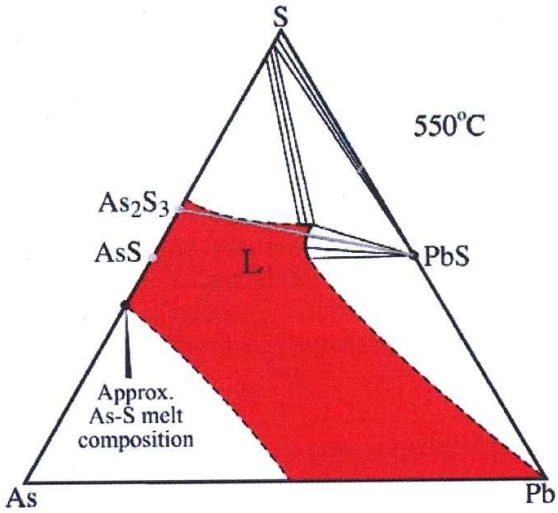

Figure 17. Isothermal section of the Pb-As-S system (data from Roland (1968) [51] and Massalski et al. (1990)), compositions are in mol. % [55].

Table 8. Reactions reported by Roland [51] while determining the composition of jordanite using the silica-tube experiment. Reactants were melted to a homogenous liquid prior to annealing. L* refers to liquids that crystallized to $Pb_9As_4S_{15}$ and $Pb_2As_2S_5$ during quenching.

Reaction	Composition (Mol% As_2S_3)	T (°C)	Heating Time (hours)
Pb + As + S = $Pb_9As_4S_{15}$ + PbS + V	18.0	500	69
PbS + As_2S_3 = $Pb_9As_4S_{15}$ + V	18.2	500	168
Pb + As + S = $Pb_9As_4S_{15}$ + V	18.6	500	66
PbS + As_2S_3 = $Pb_9As_4S_{15}$ + L* + V	18.2	400	480
PbS + As_2S_3 = $Pb_9As_4S_{15}$ + PbS + V	15.0	400	1080
PbS + As_2S_3 = $Pb_9As_4S_{15}$ + $Pb_2As_2S_5$ + V	21.1	400	1080
Pb + As + S = PbS + $Pb_9As_4S_{15}$ + L* + V	$Pb_{28}As_{12}S_{48}$	500	48
Pb + As + S = PbS + $Pb_9As_4S_{15}$ + $L_{(\sim S(l))}$* + V	$Pb_{27}As_{12}S_{43}$	500	150

2.2.4 Zn-Pb

The Pb-Zn system has large miscibility gap in the liquid and a monotectic and eutectic reactions at lower temperatures [43, 56]. Mutual solid solubilities of Pb and Zn are essentially negligible [43, 56]. A phase diagram of the system is shown in Figure 18.

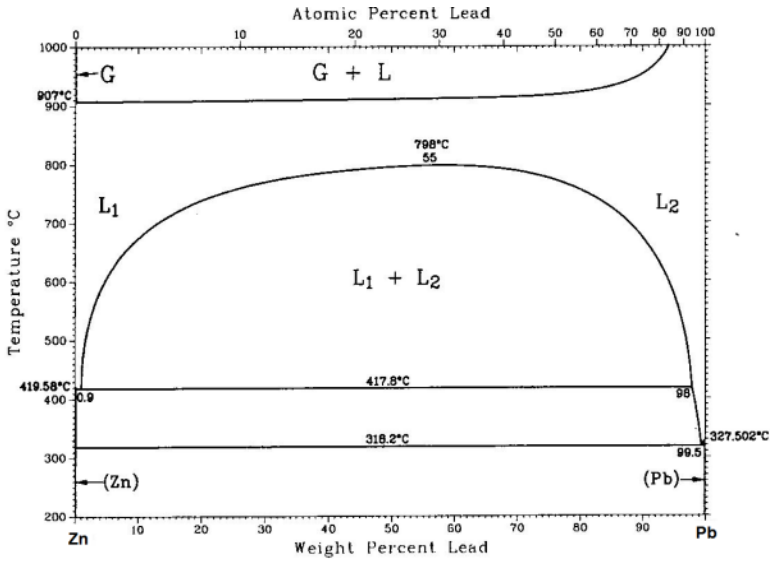

Figure 18. Phase diagram of the system Zn-Pb [57].

2.2.5 Zn-Pb-S

By using thirteen compositions of pure PbS (99.999 %) and ZnS (99.9995%) in sealed and evacuated silica capsules, and a DTA analysis with a palladium holder at rates of 5, 10, or 15 °C/min, Dutrizac (1980) [58] studied the phase relations in the binary ZnS-PbS system. He used X-ray diffraction, metallographic examination, and electron microprobe analysis to characterize the phases. His study agrees in general with Friedrich [59] but neither study agrees with the more recent work of Kerby [60]. A tentative phase diagram of the binary system is presented in Figure 19.

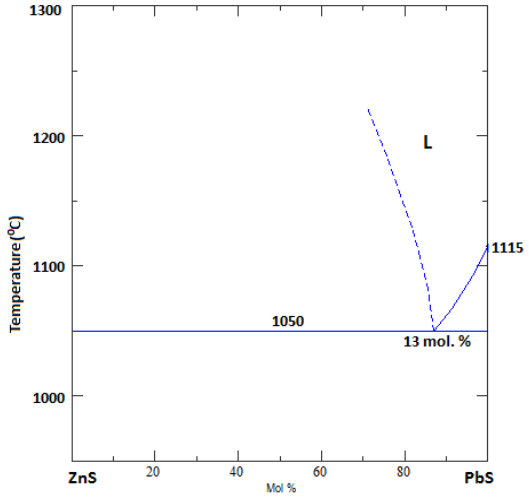

Figure 19. Phase diagram of the system ZnS-PbS [58], reassessed by [41].

2.3 The System Zn-*Cu-As-Pb*-S

In this section, phase equilibria in the systems Cu-Pb, Zn-Cu-Pb, Cu-Pb-S, Cu-Pb-As-S will be reviewed. The assemblages of equilibrium native chemical elements, binary- and ternary-phases and their solubility into one another will be discussed.

At temperatures below 900 °C, in the four-component systems Zn-Cu-Pb-S and Zn-Pb-As-S, and in the five-component system Zn-Cu-As-Pb-S no quaternary or quinary equilibrium phases are reported to exist as a mineral or synthetic phase. Furthermore, in the broader four- and five-component systems, there are less or no experimental phase equilibria studies available in the literature.

2.3.1 Cu-Pb

The melting point of pure copper is 1084.87 °C and that of pure lead is 327.50 °C [62]. They both crystallize in an fcc lattice of the same type, characterized by the Pearson sysmbol cF4 [63].

The Cu-Pb system does not have any known stoichiometric binary solid phases. Eutectic point exists at 326 °C and 99.94 wt. % Pb. Solubility of Cu in Pb(l) increases to about 2 wt. % at 700 °C and to about 7.5 wt. % at 900 °C. At monotectic temperature, 952 °C [64], a two-liquid field forms between 21 and 63 at. % Pb [65]. According to Hansen and Anderko [62], the critical point of the miscibility gap lies slightly below 1000 °C at a composition of 40 at. % Pb.

Solid solubilities of Pb in (Cu) and Cu in (Pb) are very limited [65, 66, 67, 68]. The only experimental point on the copper terminal solution is reported by Raub and Engel [69]. They reported a solid solubility of 0.09 at. % Pb at 600 °C. An assessment made by Teppo et al. [70] has shown that the solid solubility of Pb in (Cu) is very low, less than 0.4 at. %, at most at the monotectic temperature. The corresponding value in solid (Pb) is much smaller, below 0.02 at. % Cu [70]. Calculated phase diagram of the system is shown in Figure 20.

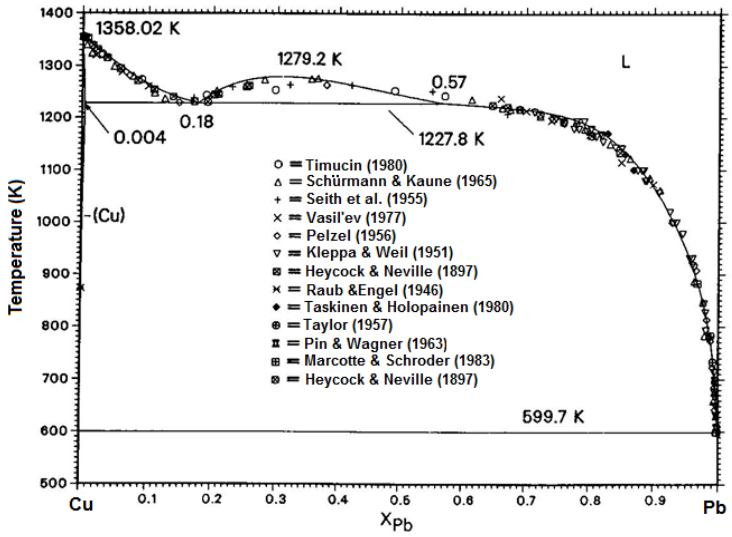

Figure 20. Calculated phase diagram for the Cu-Pb system at 500 -1400 K, with experimental points [70].

2.3.2 Cu-Pb-S

Phase relations in the Cu - S system was discussed in the previous report [3]. Summary of the identified stable phases in the system is collected to Table 9.

Craig and Kullerud [61] investigated the system Cu-Pb-S in the temperature range 200 - 1030 °C. According to their studies, above 523 °C, coexistence of PbS and Cu-sulfides is prohibited by 'central' liquid phase, a temperature significantly lower than the 540 °C given by Friedrich [71]. This sulfide liquid remains stable up to 508 ± 2 °C, the temperature at which a monotectic reaction forms PbS, a digenite solid solution, and S (l). The composition of the liquid sulfide at that monotectic temperature is 34 ± 2 wt. % Cu, 43 ± 2 wt. % Pb and 23 ± 2 wt. % S.

A ternary phase $Cu_{14}Pb_2S_{9-x}$ ($0 < x < 0.15$), which is stable between 528 ± 2 °C and 486 ± 4 °C, very close to the PbS-Cu_2S join was reported by Craig and Kullerud [61]. However, they did not find any intermediate phase along the PbS-Cu_2S join. At temperatures below 507 °C, the pure CuS and PbS phases coexist [37]. A ternary phase diagram at 510 °C and the schematic presentation for the decomposition of the phase are shown in Figure 21 and Figure 22, respectively.

Between 528 ± 2 °C, the temperature at which phase A appears, and 523 °C, the temperature at which Cu_2S-Cu_9S_5ss-PbS tie lines are established, reactions (6) to (9) take place. As temperature decreases reactions take place, probably, in the order from reaction (6) to (9).

Cu_2S-Cu_9S_5ss + L → $Cu_{14}Pb_2S_{9-x}$ (0 < x < 0.15) (6)

Cu_2S-Cu_9S_5ss + L → $Cu_{14}Pb_2S_{9-x}$ (0 < x < 0.15) + Pb(l) (7)

Pb(l) + L → $Cu_{14}Pb_2S_{9-x}$ (0 < x < 0.15) +PbS (8)

$Cu_{14}Pb_2S_{9-x}$ (0 < x < 0.15) + L → PbS + Cu_2S-Cu_9S_5ss (9)

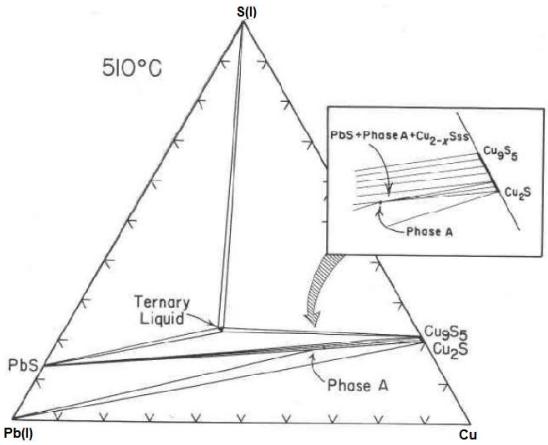

Figure 21. Phase relations in the condensed Cu-Pb-S system at 510 °C. Relations surrounding phase A ($Cu_{14}Pb_2S_{9-x}$ (0 < x < 0.15)) are magnified, schematically in the insert [61].

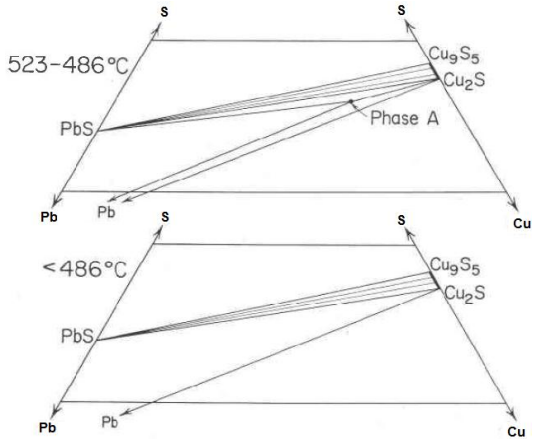

Figure 22. Schematic presentation of the decomposition of phase A to PbS + Cu_2S-Cu_9S_5ss +Pb(l) at 486 °C [61].

Reactions (8) and (9) represent invariant points whereas reaction (6) represents a singular point [61]. Between about 435 and 271 ± 5 °C, stable assemblages in the system are: PbS-Cu_2Sss-Pb, PbS-Cu_2Sss-Cu_9S_5ss and PbS-Cu_9S_5ss-CuS. Below 271 °C the following reaction takes place [61]: Cu_2S-Pb → PbS + 2Cu.

Wagner and Wagner [80], in an electrochemical study, determined that the following invariant reaction to occur at 279 ± 4 °C:

$$2Cu + PbS \rightarrow Cu_2S + Pb \quad (10)$$

Phase relations below 200 °C contain copper sulfides such as covellite (CuS) and djurleite ($Cu_{1.96}S$).

Table 9. Summary of minerals and compounds in the system Cu-Pb-S [42, 61, 81].

Composition	Mineral name	Thermal stability:	Ref.
Cu_2S (monoclinic)	Chalcocite	103	[81]
Cu_2S (hexagonal)	-	103 -~435	
Cu_2S (cubic)	-	~435 - 1129	
Cu_2S (tetragonal)	-	> 1 Kbar	
$Cu_{1.8+x}S$(cubic)	high digenite	83 - 1129	
$Cu_{1.97}S$ (orthorhombic)	djurleite	93	
$Cu_{1.8}S$(cubic)	digenite	76 - 83	
$Cu_{1.78}S$ (monoclinic)	roxbyite	-	
$Cu_{1.75}S$ (orthorhombic)	anilite	76	
$Cu_{1.60}S$ (cubic)	geerite	-	
$Cu_{1.4}S$ (hexagonal-R)	spionkopite	-	
Cu_9S_8 (hexagonal-R)	yarrowite	up to 157	
CuS (hexagonal-R)	Covellite	up to 507	
CuS_2 (cubic)	villamaninite	-	
PbS	Galena	1115	[42]
$Cu_{14}Pb_2S_{9-x}$ $(0 < x < 0.15)$	-	528 ± 2 (T_{min}: 486 ± 4)	[61]

Using eleven compositions of unspecified purity, Kopylov et al. (1976) [82] studied phase relations in the $Cu_{2-x}S$-PbS system. They used DTA, microscopic examination, and X-ray diffraction to determine the compositions in the binary system; their proposed phase diagram is shown in Figure 23. The phase $Cu_{14}Pb_2S_9$, equivalent to the phase in Table 9, is the same as phase A reported by Craig and Kullerud [61]. However, they indicated that the phase is not stable if the copper sulfide is richer in S (e.i., $Cu_{2-x}S$) than Cu_2S (chalcocite). Density of the ternary phase measured on a Berman balance is 8.42 ± 0.08 g/cm^3 [82].

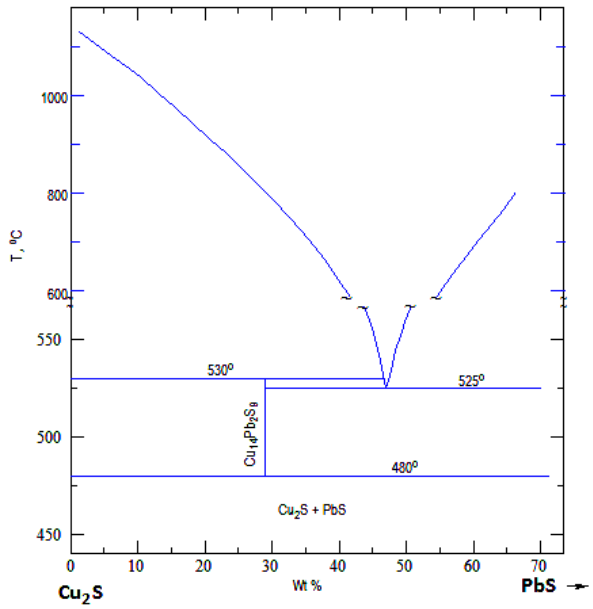

Figure 23. Phase diagram of the system $Cu_{2-x}S$-PbS [41] (data from [82]).

Johto's [83] themoanylitic studies on the pseudo binary system Cu_2S-PbS suggested that the eutectic point to be at 520 ± 2 °C and about 50 wt. % PbS, in agreement with the works of Kopylov et al. [82] and Goto and Ogawa [85], as illustrated in Figure 24.

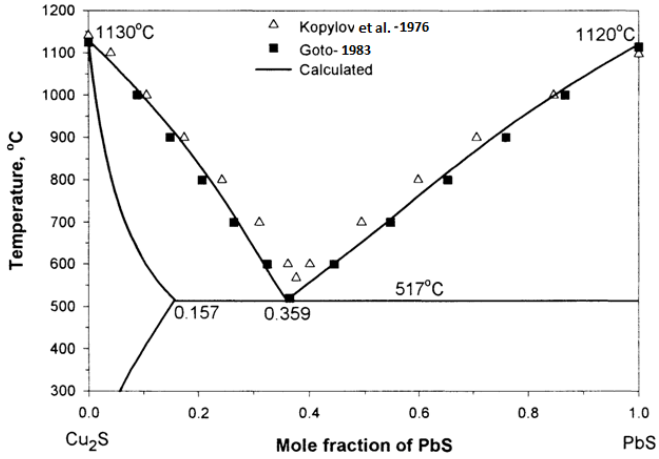

Figure 24. Calculated pseudobinary phase diagram of the system Cu_2S-PbS with experimental points [84].

Above 600 °C, the system Cu-Pb-S is dominated by two-liquid fields, in both the S- and metal-rich portions [61]. Cho [86] and Cho & Won [87] experimentally investigated the system Cu-Pb-S in the temperature range 600 – 1250 °C. Cho [86] determined isothermal phase relations at 600 °C

and 700 °C, as shown in Figure 25 and Figure 26, respectively. His studies have shown that phase relations at 600 °C and 700 °C are very similar, with some variations in the compositional range of the phase regions.

Cho & Won [87] reported phase diagram of the system Cu-Pb-S at temperatures 800 °C and 900 °C to be very similar. An isothermal phase diagram at 800 °C is illustrated in Figure 27. The three phase region; sulfide (l) + a single sulfide-rich phase + PbS, observed in the isotherms at 600 °C and 700 °C are not stable phase region of the isotherm at 800 °C, as shown in Figure 27.

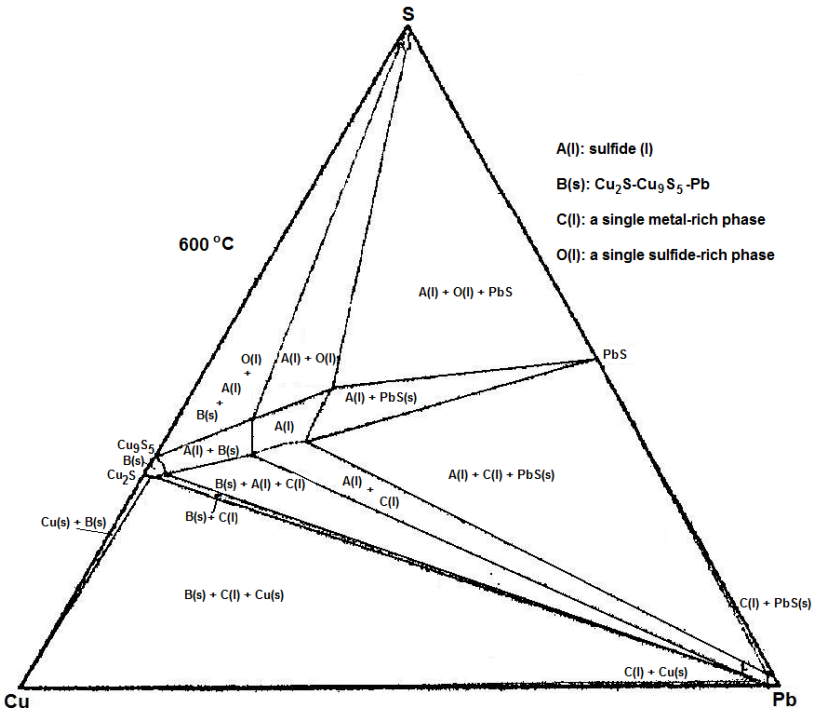

Figure 25. Phase relation in the system Cu-Pb-S at 600 °C, modified from Cho [86].

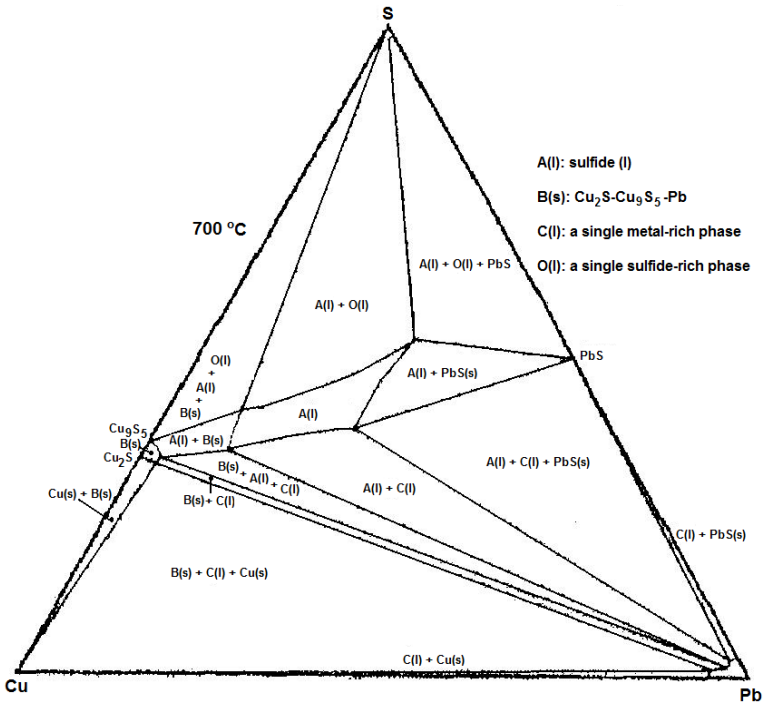

Figure 26. Phase relation in the system Cu-Pb-S at 700 °C, modified from Cho [86].

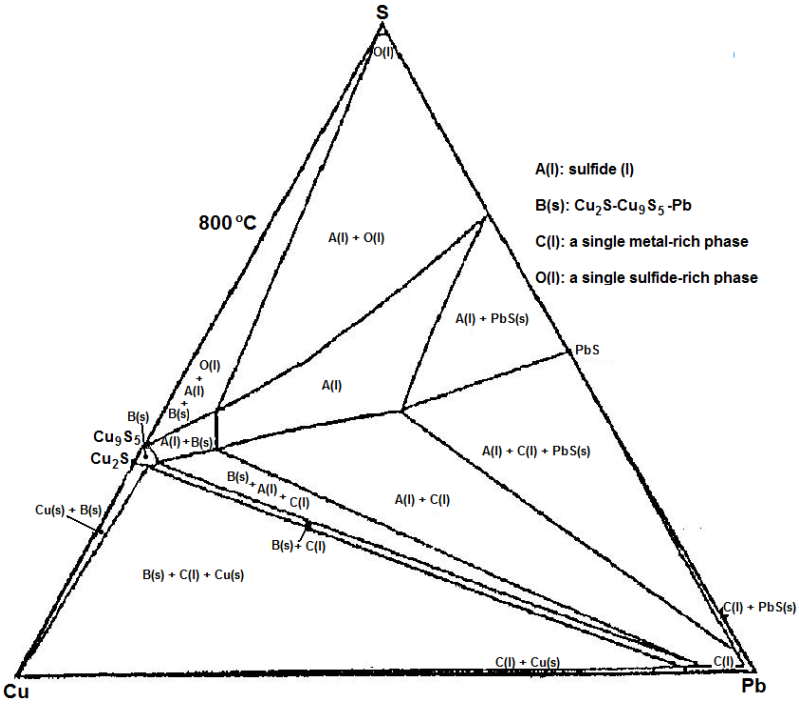

Figure 27. Phase relation in the system Cu-Pb-S at 800 °C, modified from Cho & Won [87].

Grant and Russel [88] have investigated the effect of copper on the activity coefficient of sulfur in the Pb-rich solutions over the temperature range of 500 – 900 °C. To represent the limiting activity coefficient of sulfur in Pb(l), $\gamma^{o}_{S(l)}$, and the Gibbs energy interactions, $\gamma^{o}_{S(l)}$ and $\gamma^{o}_{S(l)}$, they derived the following equations (T: 500 – 900 °C):

$$ln\gamma^{o}_{S(l)} \approx -0.283 - \frac{5460}{T(K)} \quad (11)$$

$$ln(-\varepsilon^{Cu}_{S}) \approx -1.285 - \frac{4769}{T(K)} \quad (12)$$

$$\varepsilon^{S}_{S} \approx 0 \quad (13)$$

The value $\varepsilon^{Cu}_{S}(T = 500\ °C) \approx -55$ determined by Twidwell and Larson [89] is in good agreement with that obtained from the above equation (12).

2.3.3 Cu-Pb-As-S

While studying arsenopyrite-bearing massive Zn-Pb deposits, Tomkins et al. [55] reported that they encountered seligmannite ($PbCuAsS_3$) as an inclusion in quartz veins, as depicted in Figure 28. It is stable up to 460 °C. Its standard Gibbs energies of formation and formation energies via the sulfidation reactions of Cu_2S, PbS and As are presented in chapter 3 (Table 11 and Table 12), respectively.

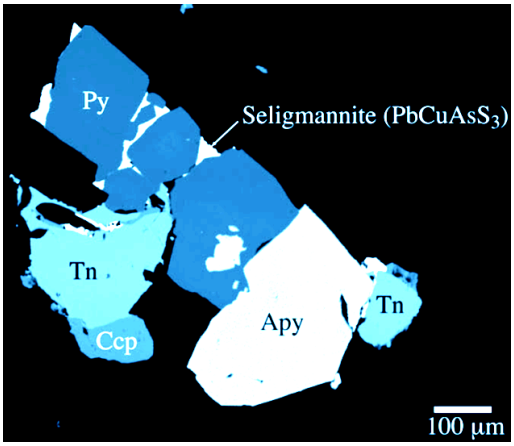

Figure 28. An element-distribution map of a mineral sample from the Osborne lake deposit showing an aggregate of pyrite(Py), arsenopyrite(Apy, FeAsS), tennantite (Tn), seligmannite(there was a trace of PbS in seligmanite) and chalcopyrite(Ccp, $CuFeS_2$), arsenic added digitally to a BSE (Back-scatter detector) image [55].

2.3.4 Zn-Cu-Pb

Thermodynamic assessment of the Zn-Cu-Pb system has been made by Jantzen and Spencer (1998) [72] and Miettinen et al. (2010) [73]. They presented an isopleth of the Zn-Cu-Pb system in the Pb-poor region, as shown in Figure 29. The liquidus projection and primary phase map of the system is shown in Figure 30.

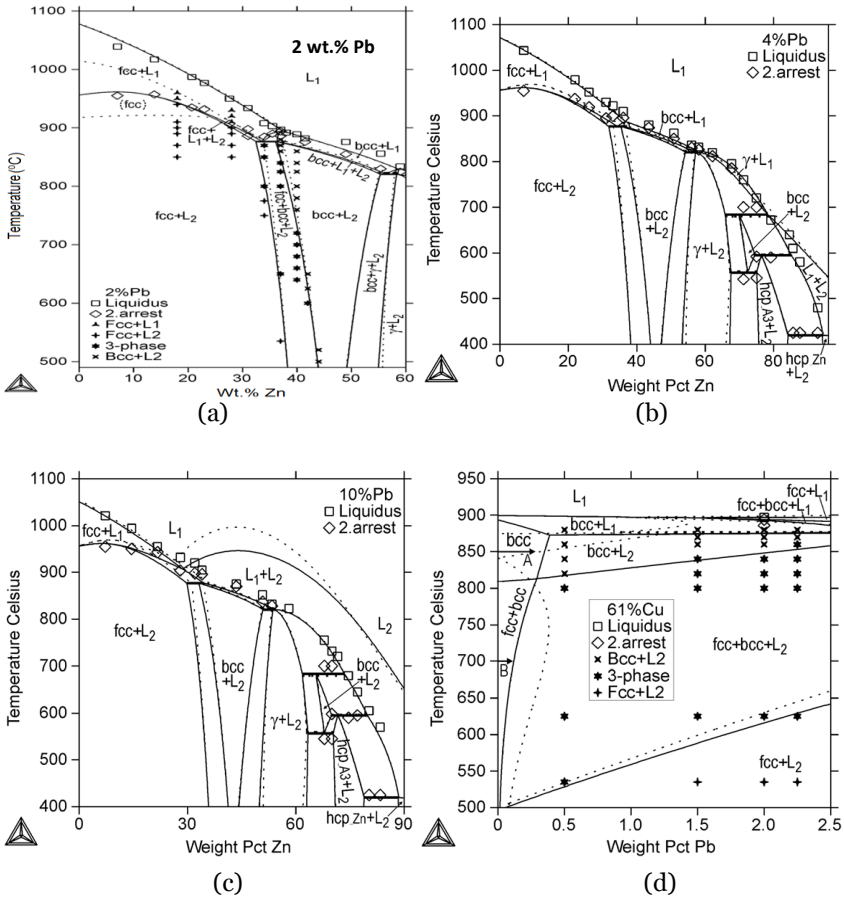

Figure 29. Calculated isopleths of the Cu-Pb-Zn system together with experimental data points [74, 75, 76] at a) 2 wt. % Pb in the copper-rich portion, b) 4 wt. % Pb, c) 10 wt. % Pb and d) 61 wt. % Cu, arrows A and B show experimentally determined [77, 78] extensions of the bcc region at 850 °C and the fcc + bcc region at 700 °C, respectively. Solid lines refer to the calculations of assessment [72] and dotted lines to [73].

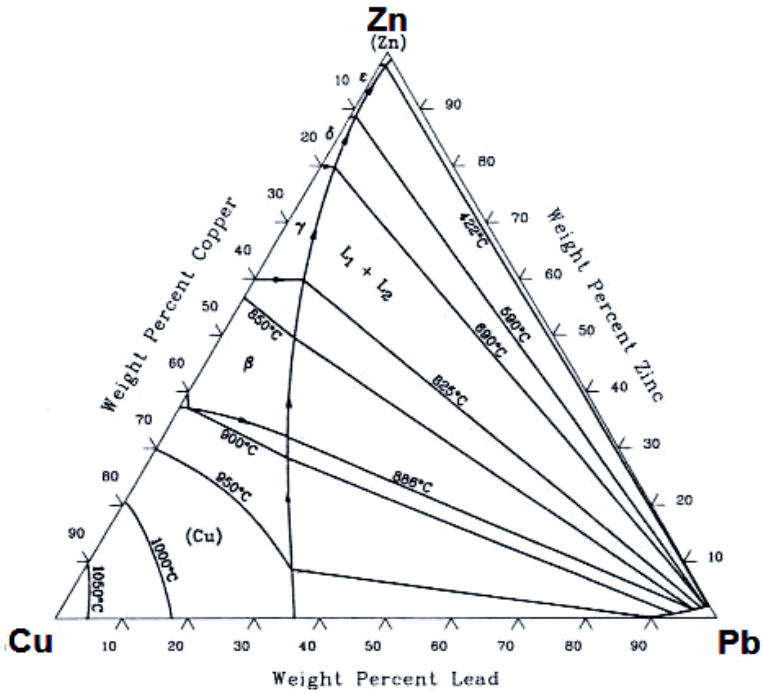

Figure 30. Cu-Zn-Pb liquidus projection (Okamoto, 1992) [79].

3 Review of Thermodynamic Data

Most sulfosalts may be regarded as intermediate phases on the joins between simple sulfide components (e.g., sulfosalts in the system Pb-Bi-S lie on the join PbS-Bi_2S_3). Therefore, the chemical compositions of the sulfosalts are, in general, stoichiometric, having formula consistent with normal valences of the elements. Furthermore, many of the structures are similar to those of the component simple sulfides (e.g., galena-like and stibnite-like layers in lead sulfantimonides) [38].

Arsenic which is known for forming both volatile and condensed compounds can be eliminated in the processing of ore minerals and concentrates by volatilization [90, 91]. Gibbs energies of pure As species and some of its compounds (mostly sulfides) are presented in Table 10.

Table 10. Compilation of experimentally determined thermodynamic data for arsenic, arsenic sulfides and arsenides.

Reaction	$\Delta G_{T(K)}$ (J/mol)	T(K)	Ref.
As(s) = As(l)	23645 - 21.7·T	1098	[92]
As(s) = As(g)	287997 – 157.1·T + 5.901·T·logT + 2.626·10^{-3} ·T^2	298- 1600	[93]
2As(s) = As_2(g)	193580 – 244.3·T + 24.88·T·logT + 4.670·10^{-3}·T^2	298- 1600	
3As(s) = As_3(g)	219490 – 272.8T + 22.64 ·T·logT + 7.027·10^{-3}·T2	298- 1600	
4As(s) = As_4(g)	160700 – 279.8·T + 31.07·T·logT + 9.317·10^{-3}·T^2	298- 1600	
4As(s) + 3S_2(g) = 2As_2S_3(l)	-491870 + 428·T	585 – 718	[94]
4As(s) + 2S_2(g) = As_4S_4(l)	-350650 + 270·T	580 – 718	
2As_2(g) + 3S_2(g) = As_4S_4(g)	-622920 + 461·T	298–1000	
As_2(g) + S_2(g) = 2AsS(g)	36410 – 22.2·T	298 – 1000	[95]
4As(s) + 3Cu(s) = Cu_3As (s)	-108480 + 1.4·T	298 – 1098	[92, 96]
As_4(g) + 6Zn(l) = 2Zn_3As_2	-271960 – 346·T + 144·T·logT	613 – 853	[14]

Craig & Barton [38] and Lynch [90] compiled preliminary estimates on the thermodynamic properties of sulfosalts as shown in Table 11. The former authors have also estimated the Gibbs energies for sulfidation reactions shown in Table 12. The thermochemical data could be used in the

prediction of the general behavior of sulfosalts and the stabilities in dry systems, as well as in improving procedures for extraction and refining of valuable metals from sulfide ores [38]. However, they mentioned the fact that the data may not be sufficiently precise to predict the fine structures of the complex phase diagrams.

Table 11. Estimates of thermodynamic properties of some minerals and compounds in the system Zn-As-Cu-Pb-S. Standard states: S_2(g), As(s), Pb(s), Cu(s) and Zn(s).

Composition (mineral name)	$T_{stability}$ (°C)	$G_{T°(K)}$ (Cal./f.unit)	T'(°C)	Ref.
Cu_3AsS_4 (Luzonite)	25 – 300	-104458 + 56.16·T	25-600	[22], effect of transition neglected.
Cu_3AsS_4 (Enargite)	300 – 665			[22, 105], effect of transition neglected.
$Cu_{21}As_{12}S_{31}$	300 – 578	-	-	[22]
$Cu_{12}As_4S_{13}$ (Tennantite)	25 – 665	-355468 +172.28·T	25-600	[22], composition not well represented by formula
$Cu_6As_4S_9$ (Sinnerite)	25 – 489	-236340 +136.83·T	25-489	[22]
$Pb_9As_4S_{15}$ (Gratonite)	25 – 250	- 475410 + 250.29·T	25-250	[51], effect of transition neglected.
$Pb_9As_4S_{15}$ (Jordanite)	250 - 549	-	-	[51]
$Pb_2As_2S_5$ (Dufrenoyesite)	25 - 485	-143980 + 86.06·T	25-485	[51]
$Pb_3As_4S_9$ (Baumhauerite)	25 - >500	-229470 + 157.26·T	25 - 500	[38]
$PbAs_2S_4$ (Sartorite)	25 - ?	-106490 + 71.48·T	25 - ?	[38], formula uncertain
$Pb_{13}As_{18}S_{40}$ (Rathite I)	25 - ?	-1108370 + 700.38·T	25 - ?	[38], formula uncertain
$Pb_9As_{13}S_{28}$ (Rathite II)	25 - ?	-775460 + 482.00·T	25 - ?	[38], formula uncertain
$CuPbAsS_3$ (Seligmannite)	25 - 460	-88380 + 45.68·T	25 - 327	[117]
		-89530 + 49.10·T	327- 460	
$Cu_6Zn_3As_4S_{12}$ (Nowackiite)	25 - ?	-420431 + 190.58·T	25 - ?	[38]
$Cu_{10}Zn_2As_4S_{13}$ (Zn-tennantite)	25 – 420	-2,119,070 + 908.3·T	25 – 420	[40]
	420– 602	-2,130,050 + 923.9·T	420 -602	

Table 12. Selected Gibbs energies of sulfidation reactions as suggested by Craig and Barton [38]. Not all sulfidation reactions are known to represent stable equilibria. The luzonit/inargite formation through the sulfidation of tetrahedrite was taken from Maske & Skinner [22] and Wernick & Benson [105].

Sulfidation reaction	$G_{T(K)}$(Cal./formula unit)	T(°C)
$⅔Cu_{12}As_4S_{13} + S_2(g) = \frac{8}{3}Cu_3AsS_4$	-41576 + 34.91·T	25 - 500
$3PbS + \frac{4}{3}As + S_2(g) = ⅓Pb_9As_4S_{15}$	-46000 + 31.71·T	25 - 500
$⅗Pb_9As_4S_{15} + 4AsS + S_2(g) = \frac{18}{5}Pb_2As_2S_5$	-41800 + 27.59·T	25 - 281
$⅗Pb_9As_4S_{15} + 4(S\text{-}As)_{(liq.)} + S_2(g) = \frac{18}{5}Pb_2As_2S_5$	-45800 + 33.39·T	281 - 450
$6Pb_2As_2S_5 + 4AsS + S_2(g) = 4Pb_3As_4S_9$	-41800 + 30.68·T	25 - 281
$6Pb_2As_2S_5 + 4(S\text{-}As)_{(liq.)} + S_2(g) = 4Pb_3As_4S_9$	-45800 + 36.48·T	281 - 500
$⅔Cu_2S + \frac{4}{3}PbS + \frac{4}{3}As + S_2(g) = CuPbAsS_3$	-46000 + 30.97·T	25 - 104
	-46213 + 32.59·T	104 - 435
$Cu_2S + ZnS + \frac{4}{3}As + S_2(g) = ⅓Cu_6Zn_3As_4S_{12}$	-46064 + 29.82·T	25 – 104
	-46984 + 32.26·T	104 - ?

3.1 The Effect of Small Amounts of Impurities on T_m

Natural sulfides and sulfosalts or their assemblages harbor small amounts of impurities that may directly affect the thermodynamic properties of the pure sulfides and sulfosalts or their assemblages discussed above. Altering the melting temperature of the minerals is one of the many impacts.

The melting temperatures of some sulfide minerals and their assemblages are collected to Table 13. According to Mavrogenes et al. [102], addition of 1 wt. % Ag_2S into the system FeS–PbS–ZnS decreases the minimum melting point of the system by 28°C; details of some of their findings are shown in Table 13. Similarly, addition of small amounts of Pb will significantly decrease the melting temperature of the assemblage skinnerite (Cu_3SbS_3) + chalcocite (Cu_2S) from 608 °C (Skinner et al. 1972 [24]) to 477 °C (Hoda & Chang [110]) [23]. While studying Zn-Pb-rich ore deposits, Frost et al. [23] concluded also that galena-bearing assemblages melt at a lower temperature than galena-free assemblages dominated by chalcopyrite.

At temperatures below 900 °C, increased fractions of Fe in sulfide-assemblages may increase the temperature at which the assemblages melt. Frost et al. [23] reported the assemblage bornite (Cu_5FeS_4) + galena (PbS) to melt at 609 °C, whereas the assemblage chalcopyrite ($CuFeS_2$) + galena (PbS), which has relatively higher fraction of Fe, melts at 630°C. In an

attempt to stabilize the ternary Cu-Pb-S melt below 508 ± 2 °C, the lowest temperature at which the ternary liquid exists, Craig & Kullerud [61] conducted experiments by adding 5 wt. % $Fe_{1-x}S$ (61.5 wt. % Fe) and 7 wt. % ZnS to samples of composition 34 wt. % Cu, 43 wt. % Pb, and 23 wt. % S, which is the composition of the ternary liquid with the lowest melting temperature. At 511 °C, they reported the samples which contained $Fe_{1-x}S$ had only small amounts of liquid sulfide, whereas the samples which contained ZnS were almost totally melted. However, heating at $T \leq 507$ °C in both cases, for half an hour, didn't result in any melt formation. Based on these results, Craig & Kullerud [61] concluded that the presence of small amounts of Fe or Zn in the system Cu-Pb-S does not at least decrease the melting temperature, 508 ± 2 °C.

The presence of low temperature-melting chalcophile elements such as As, Sb, Bi, Pb, Se, Hg, Te and Ag reduces the temperature at which sulfide's partial melting starts [23, 102]. However; the amount, the form of presence and interaction with the host system could determine the intensity of the effect.

Table 13. Melting temperatures of some of the sulfide minerals and their assemblage [21, 23, 37, 41, 54, 55, 98, 99, 100, 101].

Mineral or assembledge	Chemical Formula/ mineral association (wt. %)	T_m (°C) at 1 bar	Ref.
Sartorite	$PbAs_2S_4$	305	[54]
Baumhauerite	$Pb_3As_4S_9$	458 (incongruent)	
Jordanite	$Pb_9As_4S_{15}$	549 (incongruent)	
Orpiment + galena	(44 %)As_2S_3 + PbS	300	
Orpiment	As_2S_3	310	[64]
Galena	PbS	1115	[35]
		1114	[59]
Galena - chalcocite	PbS + Cu_2S	508 ± 2	[61]
Galena + bornite	PbS + Cu_5FeS_4	609	[23]
Galena + chalcopyrite	PbS + $CuFeS_2$	630	

Table 13 (continue)

Galena - sphalerite	(8 wt. %)ZnS + (92 wt. %)PbS	1040	[71]
Galena-sphalerite-pyrrhotite	(62.5 wt. %)PbS–(30.5 wt. %)FeS–(7 wt. %)ZnS	800 ± 3 (eutectic at 1bar)	[102]
	(61.9 wt. %)PbS–(30.2 wt. %)FeS–(6.9 wt. %)ZnS-(1 wt. % Ag_2S)	772 ± 2 (eutectic at 1bar)	
Galena-sphalerite-pyrrhotite	(62.5 wt. %)PbS–(30.5 wt. %)FeS–(7 wt. %)ZnS	~ 830 (eutectic at 5Kbar)	
	(61.9 wt. %)PbS–(30.2 wt. %)FeS–(6.9 wt. %)ZnS-(1 wt. % Ag_2S)	< 810 (eutectic at 5 Kbar)	
	(62.5 wt. %)PbS–(30.5 wt. %)$Fe_{0.96}S$–(7 wt. %)ZnS	~ 813 ± 5 (eutectic at 5 Kbar)	
	(61.9 wt. %)PbS–(30.2 wt. %)$Fe_{0.96}S$–(6.9 wt. %)ZnS-(1 wt. % Ag_2S)	~ 795 ± 5 (eutectic at 5 Kbar)	
Tennantite	$Cu_{12}As_4S_{13}$	665	[22, 116]
Tennantite	Cu_3AsS_3	640	[105]
		656	[103]
		637	[109]
		670	[108]
Tennantite	$Cu_{12.31}As_4S_{13}$	665	[22]
Enargite	Cu_3AsS_4	665	[105]
		689	[106]
Enargite	Cu_3AsS_4= L Cu_3AsS_4= $Cu_{12+x}As_{4+y}S_{13}$ + L	672 672	[22, 106]
Enargite	Cu_3AsS_4= $Cu_{12+x}As_{4+y}S_{13}$ + L	642	[107]
Lautite	CuAsS ⇋ $Cu_{12+x}As_{4+y}S_{13}$ + As + L	574	[21]
Lautite	CuAsS ⇋ As + L	596	[21]

4 Summary and Conclusions

Phase relations and thermodynamics of some equilibrium phases in the systems Zn-Cu-As-S, Zn-Pb-As-S and Zn-Cu-As-Pb-S were compiled and reviewed, based on available literature. Experimental phase equilibria studies in the broader quaternary and quinary systems are rare or unavailable in the literature. Phase relations and stabilities of some binary and ternary phases in the multi-component systems are relatively well-established. Identified binary and ternary phases as well as solubility limits and their coexistence (including the native chemical elements) were discussed. Summary of ternary equilibrium phases reviewed in the system Zn-As-Cu-Pb-S are given in the Appendix.

Finally, the Gibbs energies of formation of some stable phases in the system Zn-Cu-As-Pb-S and the effect of small amounts of impurities on the melting temperatures of the pure sulfides/sulfosalts and their assemblages were compiled and reviewed.

The studies have shown that the amount of As to significantly lower the melting temperatures of either pure sulfides/sulfosalts or their assemblages, as shown in Table 13. For instance; $PbAs_2S_4$ (28.6 at. % As) melts at about 305 ^oC, whereas $Pb_3As_4S_9$ (25 at. % As) melts incongruently at about 458 ^oC and $Pb_9As_4S_{15}$ (14.3 at. % As) melts incongruently at about 549 ^oC. CuAsS (33.33 at. % As) melts at 596 ^oC whereas enargite, Cu_3AsS_4 (12.5 at. % As), melts at 672 ^oC. This may also suggest that the effect of increasing As on lowering the melting temperature of sulfosalts is more severe in Pb-bearing systems than Cu-bearing systems.

Acknowledgements

The authors are grateful to Improved Sulfide Smelting (ISS) project of the ELEMET program and Tekes, the Finnish Funding Agency for Technology and Innovation, for financial support. This work was made as a sub task of ISS, supported financially also by Boliden Harjavalta Oy, Boliden Kokkola Oy, Norilsk Nickel Finland Oy and Outotec (Finland) Oy.

References

1. Craig, J. R. & Kullerud, G. The Cu-Zn-S System, Mineral. Deposita (Berl.) 8 (1973), pp. 81 – 91.

2. Latvalahti, U.: Cu-Pb-Zn Ores in the Aijala-Orijarvi Area, Southwest Finland, Economic Geology, Vol. 74 (1979), pp. 1035 - 1059.
3. Tesfaye Firdu, F. & Taskinen, P.: Sulfide Mineralogy - Literature Review, Aalto University Publications in Materials Science and Engineering, Espoo, TKK-MT-214 (2010), 51 p. ISBN 978-952-60-3271-9.
4. Hietanen, P.: Epäpuhtaussulfidisysteemien tasapainot ja termodynamiikka sekä Ag-Te-systeemin tutkiminen emf-tekniikalla, Diplomityö, Aalto-yliopiston teknillinen korkeakoulu, Materiaalitekniikan tutkinto-ohjelma, Espoo (2010), 66 s.
5. Tesfaye Firdu, F. & Taskinen, P.: Thermodynamics and Phase Equilibria in the (Ni, Cu, Zn)-(As, Sb, Bi)-S Systems at Elevated Temperatures (300 – 900 ^{o}C), Aalto University Publications in Materials Science and Engineering, Espoo, TKK-MT-216 (2010), 51 p. ISBN 978-952-60-3271-9.
6. Barton, P. B., Jr.: Thermochemical study of the system Fe-As-S, Geochimica et Cosmochimica Acta, 33 (1969), pp. 841 – 857.
7. Morgan, S.W.K.: Zinc and Its Alloys and Compounds, Ellis Horwood Series in Industrial Metals, ISBN 0-470-20213-0 (1985), 238 p.
8. LENNTECK, Water Treatment and Purification, URL address: http://www.lenntech.com
9. Heike, W.: Das Erstarrungsbild der Zink-Arsen-Legierungen. Zeitschrift für anorganische und allgemeine Chemie, 118 (3) (1921), pp. 264 – 268.
10. Lazarev, V.B., Guskov, V. N. & Greenberg, J. H.: P-T-X Phase equilibria in the system Zn-As, Mater. Res. Bull., 16(9) (1981), pp. 1113 – 1120.
11. Friedrich, K. and Leroux, A.: Zinc and Arsenic, Metallurgie, 3(14) (1906), pp. 477 – 479 (in German).
12. Pietraszko, A. and Łukaszewicz, K.: Thermal expansion and phase transitions of Cd_3As_2 and Zn_3As_2, Physica Status Solidi (a), vol. 18, Issue 2 (1973) pp. 723 –730.
13. Clark, J. B. and Range, K. J.: High Pressure Reactions in the. Systems Zn_3As_2-As and Cd_3As_2-As, Z. Naturforsch. B, 30 (5) (1976), pp. 688 – 695.
14. Schoonmaker, Richard C. and Lemmerman, Keith J.: Vaporization of Zn_3As_2, Journal of Chemical and Engiineering Data, vol. 17, No. 2 (1972), pp. 139 – 143.
15. Okamoto, H.: As-Zn (Arsenic-Zinc), Binary Alloy Phase Diagrams, ASM, Vol. 3 (1992), 104 p.

16. Alan, H. Clark: Arsenian sphalerite from Mina Alcaran, Pampa Larga, Copiapo, Chile. The American mineralogist. vol. 55. 1970. pp. 1794-1797.
17. Skinner, B. J., and Barton, P. B., Jr.: The substitution of oxygen for sulfur in wurtzite and sphalerite: Am. Mineralogist, v. 45 (1960), p. 612-625.
18. Frondel, Clifford: Voltzite, The American Mineralogist, vol. 52 (1967), pp. 617-634.
19. Olekseyuk, I. D. & Tovtin, N. A. Phase equilibria and glass formation in the Zn-As-S system. Russian Journal of Inorganic Chemistry, 32 (10). 1987. pp. 1490-1492.
20. Shie, Bo-rung, Chen, Sinn-wen & Wang, Jinn-lung: Interfacial stability of the As –Se-S/ZnS, As-Se-S/ZnSe, As-Se-Tl/ZnS, As-Se-Tl/ZnSe, and related systems, Journal of Non-Crystalline Solids, 231 (1998), pp. 240 – 250.
21. Müller, A. Reaktivität im System Kupfer-Arsen-Schwefel und in den Entsprechenden Randsystemen. Ph.D. Thesis. Universität Osnabruck, Fachbereich Biologie/Chemie. 2000. 182 P.
22. Maske, S. and Skinner, B.J.: Studies of the sulfosalts of copper: I, Phases and Phase Relations in the System Cu-As-S. Economic Geology, 66 (1971), pp. 901–918.
23. Frost, Ronald B., Mavrogenes, John A. & Tomkins, Andrew G.: Partial Melting of Sulfide Ore Deposites During Medium and High-Grade Metamorphism, The Canadian Mineralogist, Vol. 40 (2002), pp. 1-18.
24. Skinner, B.J., Luce, F. & E.M.: Studies of the sulphosalts of copper III. Phase relations in the system Cu-Sb-S. Econ. Geologist, 67 (1972), pp. 924-938.
25. Ralph Hultgren and Pramod D. Desai: Selected Thermodynamic Values and Phases Diagrams for Copper and Some of Its Binary Alloys, Incra Monograph I, The Metallugy of Copper (1971), 204 p.
26. Gokcen, N. A.: As-Pb (Arsenic-Lead), Binary Alloy Phase Diagrams, ASM, 2nd edition, vol. 1 (1992), pp. 306 - 308.
27. Davies, R.H. et al. (2002): MTDATA-thermodynamic and phase equilibrium software from the National Physical Laboratory. CALPHAD, 26, 2, 229-271.
28. Gisby, J. et al. (2007): Predicting phase equilibria in oxide and sulphide systems. EMC European Metallurgical Conference, June 11-14, Düsseldorf, Germany. Vol. 4, pp. 1721-1736. ISBN 978-3-940276-07-0.
29. Miodownik, A. P.: Cu-Zn (Copper-Zinc), Binary Alloy Phase Diagrams, 2nd edition, vol.2 (1990), pp. 1508 – 1510.

30. Fleet, Michael.: Phase Equilibria at High Temperature, Sulfide Mineralogy and Geochemistry, Reviews in Mineralogy and Geochemistry, vol. 61 (2006), pp. 365 - 419.
31. Scott, S. D. and Barnes, H. L.: Sphalerite-Wurtzite Equilibria and Stoichiometry, Geochim. Cosmochim. Acta 36 (1972). pp. 1275 – 1295.
32. Wiggins, L. B. and Craig, J. R.: Reconnaissance of the Cu-Fe-Zn-S system; sphalerite phase relationships, Economic Geology, vol. 75; no. 5 (1980), pp. 742 – 751.
33. Scott, S.D.: Chemical behavior of sphalerite and arsenopyrite in hydrothermal and metamorphic environments, Mineralogical. Magazine, vol. 47 (1983), pp. 427-435.
34. Clark, A. H. & Sillitoe, R. H.: Cuprian sphalerite and a probable copper-zinc sulfide, Cachiyuyo de Llampos, Copiapó, Chile, The American Mineralogist , vol. 55 (1970), pp. 1021 - 1025.
35. Toulmin, P.: Effect of Cu on sphalerite phase equilibria - a preliminary report [abstr], Geological Society, Am. Bull. 71 (1960), pp. 1993.
36. Moh, G.: ExperimenteUe Untersuchungen an Zinnkiesen und analogen Germaniumverhindungen, Neues Jahrb, Mineral., Abhandl. 94 (1960), pp. 1125-1146.
37. Chang, Y.A, Neumann, J.P. & Choudary, U. V.: Phase Diagrams and Thermodynamic Properties of Ternary Copper-Sulfur-Metal Systems, Incra Monograph VII, The Metallugy of Copper (1979), 191 p.
38. Craig, J. R. and Barton Jr., P. B.: Thermochemical approximations for sulfosalts, Economic Geology 68 (1973), pp. 493 – 506.
39. Marumo, F.: The crystal structure of nowackiite, $Cu_6Zn_3As_4S_{12}$, Zeitschrift für Kristallographie: Vol. 124, No. 4-5 (1967), pp. 352-368.
40. Robert, R. Seal II, Eric J. Essene & William, C. Kelly. Tetrahedrite and Tennantite: Evaluation of Thermodynamic Data and Phase Equilibria. Canadian Mineralogist, vol. 28. 1990. pp. 725- 738.
41. ACerS-NIST, Phase Equilibria Diagrams, CD-ROM Database, Version 3.3, NIST Standard Refence Database 31, National Institute of Standards and Technology (NIST), The American Ceramic Society (2010).
42. Kullerud G., 1969, The lead-sulfur system: American Journal of Science, v. 267-A , pp. 233–256.
43. Hansen, M. and Anderko, K.: Constitution of Binary Alloys, McGraw-Hill, New York, NY (1958), pp. 1118-1121.
44. Rannikko, H., Sundström, S. & Taskinen, P. (1993): An optimised equilibrium phase diagram and solution thermodynamics of arsenic-lead alloys, Thermochimica Acta, Vol. 216, pp. 1-14.

45. Schlesinger, M.E. and Lynch, D.C.: Activity of Arsenic in Molten Lead, Metallurgical Transactions B. vol. 17B (1986), pp. 235 - 238.
46. Rapoport, E., Clark, J. B. & Richter, P. W.: Journal of Less-Common Metelas, 55 (1974), pp. 121 – 124.
47. Seljesater, K. S.: Effect of Arsenic on Dispersion-Har- denable Lead-Antimony Alloys, Trans. AIME (1929), pp. 573 – 580.
48. Heike, W.: Equilibrium Diagram of Lead-Arsenic. Alloys and the Melting Point of Arsenic, Int. Z. Metallogr., 6 (1914), pp. 49 – 183 (In German).
49. Zaleska, E.: Electrochemical Investigation of Liq- uid Lead-Arsenic Solutions, Rocz. Chem., vol. 48 (1974), pp. 195-200.
50. Suleimanov, D.M., Mamedov, A.N., & Kuliev, A. A.: Thermodynamic Properties of Pb-As Molten alloys Studied by EMF measurment Method, lzv. Vyssh. Ucheb. Zaved., Khim. Khim. Tekhnol., vol. 17 (1974), pp. 365-67.
51. Roland, G. W.: The System Pb-As-S - Composition and Stability of Jordanite, Mineral. Deposita (Berl.), Vol. 3, (1968), pp. 249 - 260.
52. Chang, L. L. Y. & Bever, J. E.: Lead Sulfosalt Minerals: Crystal Structures, Stability, Relations, and Paragenesis, Mineral Science Engineering, Vol. 5, No. 3 (1973), pp. 181 – 191.
53. Pring, A.: Disordered intergrowths in lead-arsenic sulfide minerals and the paragenesis of the sartorite-group minerals, American Mineralogist, Vol. 75 (1990), pp. 289-294.
54. Kutolglu, A.: Röntgenographische und thermische Untersuchungen im quasibinaren System PbS-As_2S_3. Neues Jahrbuch fur Mineralogie. Monatshefte 2 (1969), pp. 68-72.
55. Tomkins, Andrew G., Frost, B. Ronald & Pattison, David R.M.,: Arsenopyrite Melting During Metamorphism of Sulfide Deposits, The Canadian Mineralogist, Vol. 44 (2006), pp. 1045 – 1062.
56. R. Hultgren, R.L. Orr, P.D. Anderson, and K.K. Kelley: Selected Values of Thermodynamic Properties of Metals and Alloys, John Wiley, New York, NY (1963), pp. 910-14.
57. Massalski, Thaddeus B.: Alloy Phase Diagrams, Binary Alloy Phase Diagrams, ASM, Vol. 3 (1992), p. 104.
58. Dutrizac, J. E.: The $Fe_{1-x}S$–PbS–ZnS phase System, Canadian Journal of Chemistry, 58 [7] (1980), pp. 739-743.
59. Friedrich, K.: Die Zinkblende als Steinbildner, Metallurgie (Halle), 5 [4] (1908), pp. 114-128.
60. Kerby, R. C., Can., Mines Branch Invest. Rep., Rep. No. IR 73-49, Department of Energy, Mines, and Resources; Mines Branch, Ottawa, Canada, (1973), pp. 1-18.

61. Craig, J. R., G. Kullerud: Phase relations and mineral assemblages in the copper-lead-sulfur System. Amer. Mineral., 53 (1968), pp. 145-161.
62. Melting Points of the Elements, Bulletin of Alloy Phase Diagram, 2 (1981), p. 146.
63. Crystal Structures of Elements at 25 °C, Bulletin of Alloy Phase Diagram, 2 (1981), p. 402.
64. Hansen, M. & Anderko, K.: Constitution of Binary Alloys, McGraw-Hill, New York (1958).
65. Chakrabarti, D. & Laughlin, D.: The Cu-Pb (copper-lead) system, Bulletin of Alloy Phase Diagram, 5 (1984), pp. 503 – 511.
66. Elliot, R.: Constitution of Binary Alloys, First Supplement, McGraw-Hill, New York (1965).
67. Shunk, F.: Constitution of Binary Alloys, Second Supplement, McGraw-Hill, New York (1969).
68. Johnson, R.: Bulletin of Alloy Alloy Phase Diagram, 1 (1979), pp. 81 – 82.
69. Raub, E. & Engel, A.: Concerning the Retrograde. Saturation Curve in the Formation of Mixed Crystals Out of the Melt, Z. MetallKd., 37 (1946), pp. 76-81.
70. Teppo, O. Niemelä, J. & Taskinen, P.: The copper-lead phase diagram,Thermochimica Acta, Vol. 185, Issue 1 (1991), pp. 155-169.
71. Friedrich, K.: Metallurgie, vol. 4 (1907), pp. 671 – 673.
72. Jantzen, T., Spencer, P. J.: Thermodynamic assessments of the Cu-Pb-Zn and Cu-Sn-Zn systems, Calphad, vol. 22, No. 3 (1998), pp. 417 – 434.
73. Miettinen, J., Gandova, V., Vassilev, G.: Thermodynamic description of the Cu-Pb-Zn system, CALPHAD, 34 (2010), pp. 377 -383.
74. Parravano, N., Mazzetti, C., Moretti, R.: Gazzetta Chimica Italiana, 44 (1914), pp. 475 - 502.
75. Bauer, O., Hansen, M., Z.: Influence of a Third Element on the Constitution of Brasses. I. Lead Influence, Metallkd. 21(6) (1929), pp. 190 - 196.
76. Bauer, O., Hansen, M., Z.: Influence of a Third Element on the Constitution of Brasses. I. Lead Influence, Metallkd. 21(6) (1929), pp. 145 - 151.
77. Chang, Y.A., Neumann, J.P., Mikula, A., Goldberg, D.: The metallurgy of copper, phase diagrams and thermodynamic properties of ternary copper-sulfur-metal systems, in: INCRA Monograph, vol. VI (1979).
78. Leoni, M. & Fortina, G. Investigation on the Solubility of Lead in Alpha and Duplex Brasses and on the Effects of Small Quaternary Additions

on the Properties of these Alloys; Final Report, INCRA Project 156b/194, Univ. of Missouri-Rolla (1972), pp. 1-26.
79. Okamoto, H.: Alloy Phase Diagrams, Ternary Alloy Phase Diagrams, ASM, Vol. 3 (1992), 51 p.
80. Wagner and C. Wagner: J. Electrochem. Soc., 1957, vol. 104, pp. 509-11.
81. Fleet, M. E.: Phase Equilibria at High Temperature, Review in Mineralogy and Geochemistry, Vol. 61 (2006), pp. 265 – 419.
82. Kopylov, N. I., Toguzov, M. Z., Minkevich, S. M., Yarygin, V. I., and Kalganov, I. M.: The phase diagram of the $Cu_{2-x}S$-PbS system, Russian Metallurgy (Engl. Transl.), No. 3, (1976), pp. 170-172.
83. Johto, H.: Epäpuhtaan sinkkisulfidirikasteen Pasutuksen kemiasta, Diplomityö, Aalto-yliopiston teknillinen korkeakoulu, Materiaalitekniikan tutkinto-ohjelma, Espoo (2009), 71 s.
84. Degterov, Sergei A. and Pelton, Arthur D.: Thermodynamic Modeling of Lead Distribution among Matte, Slag, and Liquid Copper, Metallurgical and Materials Transactions B, vol. 30B (1999), pp. 1033-1044.
85. Goto, S. & Ogawa, O.: Activities of Cu, Pb and S in the ternary Cu-Pb-S system at 1473 K, Journal of MMIJ,vol. 99, no. 1150 (1983), pp. 39 – 45.
86. Cho, Tong-Rae & Won, Chang-Whan: Ternary Miscibility Gap (phase diagram) of the Pb-Cu-S System at 700 °C and 600 °C, Report of the Ind. Educ. Research Center, vol. 9, no. 1 (1986), pp. 9 – 13.
87. Cho, Tong-Rae: Ternary Miscibility Gap (phase diagram) of the Pb-Cu-S System at 900 °C, 800 °C, Report of the Ind. Educ. Research Center, vol. 8, no. 1 (1985), pp. 39 – 43.
88. Grant, R. M. & Russell, B.: A thermodynamic study of dilute sulfur and Cu-S solutions in lead, Metallurgical Transactions, vol. 1, issue 1 (1970), pp. 75-83.
89. Twidwell, L. G. & Larson, A. H.:The Influence of Additive Elements on the Activity Coefficient of Sulfur in Liquid Lead at 600 °C, Trans. Metall. Soc. TMS-AIME, vol. 236 (1966), p. 1414 - 1420.
90. Lynch, D. C.: A review of the physical chemistry of arsenic as it pertains to primary metals production, Arsenic Metallurgy Fundamentals and Applications: proceedings of a symposium sponsored by the TMS-AIME Physical Chemistry Committee, the 1988 TMS annual meeting and exhibition (1988), pp. 3 – 33.
91. Tuovinen, H. and Setälä, P.: Removal of Harmful Impurities from Iron, Copper, Nickel and Cobalt concentrates and Ores, Metallurgical

Research Center, Outokumpu Oy, 111th AIME Annual Meeting, Dallas, Texas, (1982).

92. Itagaki, K. and Nishimura, T.: Thermodynamic Properties of Compounds and Aqueous Species of VA elements, Metalllugicall Review of MMIJ, 3(2) (1986), pp. 29 – 48.
93. Lau, K. H., Lamoreaux, R. H. and Hildenbrand, D. L.: Vapor Pressure Determination of Arsenic Activity in a Molten Cu-Fe-S Matte, Metallurgical and Materials Transactions B, 14B (1983), pp. 253 – 258.
94. Mah, A. D., Thermodynamic data for arsenic sulfide reactions, Bureau of Mines Report of Investigation 8671 (1982).
95. Hino, M., Toguri, J. M. and Nagomori: The Gibbs Free Energy of Gaseous AsS, Canadian Metallurgical Quarterly, 25 (1986), pp. 195 – 197.
96. Barin, I., Knacke, O. and Kubaschewski, O.: Thermochemical Properties of Inorganic Substances, FRG: Springer-Verlag, Berlin (1977).
97. Craig, Jr. & Kullerud, G.: The Cu–Fe–Pb–S system, Carnegie Inst. Wash., Yearbook 65 (1967), pp. 344 - 352.
98. Müller, A. & Blachnik, R. Reactivity in the system copper–arsenic–sulfur I. The formation of Cu_3AsS_4, enargite. Thermochimica Acta 387.2002. pp. 153–171.
99. Müller, A. & Blachnik, R. Reactivity in the System Copper/Arsenic/Sulfur II. The Formation of CuAsS, (Lautite). Z. Anorg. Allg. Chem., 629. 2003. pp. 1833 – 1838.
100. Tatsuka, K. and Morimoto, N. Tetrahedrite Stability Relations in the Cu-Fe-Sb-S System. American Mineralogist. Vo. 62. 1977. pp. 1101-1109.
101. Andrew, G. Tomkins, David R.M. Pattision and B. Ronald Frost. On the Initiation of Metamorphic Sulfide Anatexis.Journal of Petrology. 2006. 25 p.
102. Mavrogenes, J.A., MacIntosh, I.W., and Ellis, D.J.: Partial melting of the Broken Hill galena-sphalerite ore: Experimental studies in the system PbS-FeS-ZnS-(Ag_2S): Economic Geology, vol. 96 (2001), pp. 205–210.
103. Kurz, G. & Blachnik, R.: New aspects of the system Cu-As-S , J. Less-Common Metals, 155 (1) (1989), pp. 1 – 8.
104. Rösch, H., Hellner, E.: Hydrothermale Untersuchungen am system PbS-As2S3, DIE NATURWISSENSCHAFTEN, vol. 46 (1959), 72 p.
105. Wernick, J. H. and Benson, K. E., Journal of Physics and Chemistry of Solids 3 (1957), 157 p.

106. Cambi, L. & Elli, M.: Hydrothermal processes: IX. Synthesis of Sulphides and Thiosalts of Trivalent Metals, Chim. Ind. (Milan) 49 (1967), p. 606.
107. Kurz, G., Ph.D. Thesis, Universität Siegen, 1984.
108. Kuzgibekova, K., Sivak, L.F., Isabaev, S.M.: Sulfidization of copper and iron arsenides by sulfur, Kompleksn, Ispol'z Miner, Syrya, Vol. 48 (1993).
109. Zhumashev, K.Z.: Thermodynamic functions of Cu_3AsS_3 and Cu_3AsS_4 and the vapor pressure during the dissociation of Cu_3AsS_4, Inorg. Mater. 28 (1992), p. 325-326.
110. Hoda, S. N., and Chang, L. L. Y.: Phase relations in the systems PbS-Ag_xS- Sb_xS_3 and PbS-Ag_xS-Bi2Sa: Am. Mineralogist, v. 60 (1975), pp. 621-633.
111. Gaines, R., Amer. MineraL, 42 (1957), p. 772.
112. Schüller, A. & Wohlmann, E. : Betechtinit, ein neues blei-kupfer-sulfid aus den Mansfelder Rücken, Geologie, 4 (1955), pp. 535-555.
113. Rösch, H.; Hellner, E.: Hydrothermale Untersuchungen am System PbS-As_2S_3. Naturw. 46 (1959), p. 72.
114. Le Bihan, M.-T. & Petiau, J. (1963): Contribution a l'etude structurale des cristalline de la rathite-III. C. R. Acad. Sci. 251 (20): pp. 2196-2198.
115. Burkart-Baumann, I. (1972) Vanadium: Element and geochemistry. in Fairbridge, R. W. (ed.) The Encyclopedia of Geochemistry and Environmental Sciences. Encyclopedia of Earth Sciences Series, 4A, 1234–1237, Dowden, Hutchnson & Ross Inc., Stroudsburg, Pennsylvania.
116. Bryndzia, L.T. & Davis, A.M.: Liquidus phase relations on the quasibinary join Cu_2S-Sb_2S_3: Implications for the formation of tetrahedrite and skinnerite, American Mineralogist, vol. 74 (1989), pp. 236–242.
117. Wernick, J.H., Geller, S., Benson, K.E.: New semi conductors. J. Phys. Chem. Solids 4 (1958): pp. 154-155.

Appendix

Summary on the ternary phases and their stabilities in the system Zn-Cu-Pb-As-S.

Chemical formula (mineral name)	T_{max} (°C)	References
Pb-As-S		
$Pb_9As_4S_{15}$ (Gratonite)	250	[52, 54, 113, 114,115]
$Pb_9As_4S_{15}$ (Jordanite)	549	
$Pb_2As_2S_5$ (Dufrenoysite)	485 ?	
$Pb_{19}As_{26}S_{58}$ (Rathite II)	474	
$PbAs_2S_4$(Sartorite)	305	
$Pb_3As_4S_9$(Baumhauerite)	458	[54]
Cu-As-S		
Cu_3AsS_4 (Luzonite)	275 – 320	[22], [111]
Cu_3AsS_4 (Enargite)	671	
$Cu_{24}As_{12}S_{31}$ (-)	578	
$Cu_6As_4S_9$ (Sinnerite)	489	
$Cu_{12}AsS_{13}$ (Tennantite)	665	
CuAsS (Lautite)	574	
Cu_3AsS_3 (near-Tennantite) (-)	656	[103]
$Cu_{12 \pm x}AsS_{13 \pm x}$ (Tennantite)	656	[21]
Cu-Pb-S		
$Cu_{14}Pb_2S_{9-x}$ (-)	486 - 528	[34, 61, 112]
Cu_3ZnS_4 (-)	< 200?	[34]

Increasing association of impurities such as arsenic in sulfide ores has been generating flurry of both experimental studies and compilation of thermodynamic data of sulfide systems that contain both impure elements and their compounds. For instance, Zn- and Cu-sulfides are relatively common ore minerals in most hydrothermal vein and replacement deposits. Although these sulfides may occur alone or together in the absence of other sulfides, they are most commonly encountered in complex ore assemblages in which the mineralogy is significantly altered by elements such as As, Pb, or Fe. Owing to the complexity of minerals in nature, a thorough evaluation of the thermochemistry of these complex ore minerals is essential for developing full understanding of the behavior of the impurities in existing and new sulfide ore minerals processing operations.

Aalto-ST 7/2011

ISBN: 978-952-60-4126-1 (pdf)
ISBN: 978-952-60-4125-4
ISSN-L: 1799-4896
ISSN: 1799-490X (pdf)
ISSN: 1799-4896

Aalto University
School of Chemical Technology
Department of Materials Science and Engineering
www.aalto.fi

BUSINESS + ECONOMY

ART + DESIGN + ARCHITECTURE

SCIENCE + TECHNOLOGY

CROSSOVER

DOCTORAL DISSERTATIONS